INTERNATIONAL STANDARD

ISO 21363

First edition
2020-06

Nanotechnologies — Measurements of particle size and shape distributions by transmission electron microscopy

Nanotechnologies — Détermination de la distribution de taille et de forme des particules par microscopie électronique à transmission

Reference number
ISO 21363:2020(E)

ISO copyright office
CP 401 • Ch. de Blandonnet 8
CH-1214 Vernier, Geneva
Phone: +41 22 749 01 11
Email: copyright@iso.org
Website: www.iso.org

Published in Switzerland

Contents

Page

Foreword

ISO (the International Organization for Standardization) is a worldwide federation of national standards bodies (ISO member bodies). The work of preparing International Standards is normally carried out through ISO technical committees. Each member body interested in a subject for which a technical committee has been established has the right to be represented on that committee. International organizations, governmental and non-governmental, in liaison with ISO, also take part in the work. ISO collaborates closely with the International Electrotechnical Commission (IEC) on all matters of electrotechnical standardization.

The procedures used to develop this document and those intended for its further maintenance are described in the ISO/IEC Directives, Part 1. In particular, the different approval criteria needed for the different types of ISO documents should be noted. This document was drafted in accordance with the editorial rules of the ISO/IEC Directives, Part 2 (see www.iso.org/directives).

Attention is drawn to the possibility that some of the elements of this document may be the subject of patent rights. ISO shall not be held responsible for identifying any or all such patent rights. Details of any patent rights identified during the development of the document will be in the Introduction and/or on the ISO list of patent declarations received (see www.iso.org/patents).

Any trade name used in this document is information given for the convenience of users and does not constitute an endorsement.

For an explanation of the voluntary nature of standards, the meaning of ISO specific terms and expressions related to conformity assessment, as well as information about ISO's adherence to the World Trade Organization (WTO) principles in the Technical Barriers to Trade (TBT) see www.iso.org/iso/foreword.html.

This document was prepared by Technical Committee ISO/TC 229, *Nanotechnologies.*

Any feedback or questions on this document should be directed to the user's national standards body. A complete listing of these bodies can be found at www.iso.org/members.html.

Introduction

Characterization procedures for nanoparticles often include, but are not limited to, size, shape, surface structure (or texture), and surface chemistry. These measurements, combined with phase information, such as crystalline phase, constitute the morphology of the material. This document focuses on two attributes of morphology, size and shape distributions, for discrete, agglomerated and aggregated nano-objects (materials with at least one dimension in the nanoscale, 1 nm < a length dimension < 100 nm). Transmission electron microscopy, a standard tool for measurements on the nanoscale, provides two-dimensional images of particle projections. This generic workflow for measuring and evaluating particle size and shape distributions on the nanoscale includes sample preparation, instrument factors, image capture, particle analysis, data analysis, and reporting. Seven case studies have been included to illustrate how the generic protocol can be applied to different particle morphologies and sample types. Three discrete particle test samples are reported: spheroidal (gold nanospheres), a bimodal mixture of particle sizes (colloidal silicas), and a mixture of particle shapes (gold nanorods and gold nanocubes). Two aggregate test samples are reported: amorphous aciniform aggregates (carbon black) and aggregates of primary crystallites (titania). Measurements methods are also presented for low aspect ratio samples and nanoparticles with specific crystal habits. Several of the case studies are supported by interlaboratory collaborations conducted under the guidelines of the Versailles Project on Advanced Materials and Standards (VAMAS) for interlaboratory comparisons (ILCs)[42].

Three types of size and shape descriptors are considered. Size descriptors include those determined by linear or areal measurements. Shape descriptors include elongational descriptors, such as ratios of two length descriptors, and ruggedness descriptors, which represent surface irregularities.

The protocol emphasizes qualitative and quantitative analysis of data quality by the user. Qualitative comparisons of datasets include determining the similarity or differences between single descriptor means or multivariate means. Quantitative comparisons of datasets are based on difference or similarities between the parameters of reference models fitted to descriptor distributions. At least two parameters (mean and spread) and their uncertainties are needed to define a descriptor distribution. In some cases, these two quantitative parameters and their uncertainties may not be sufficient for characterization of particle size and shape distributions. Data visualization techniques, such as residual deviation and quantile plots, and data correlations, such as pairs of size and shape descriptors or fractal analysis, can provide additional ways to evaluate and differentiate test samples. Taken together, qualitative and quantitative quality metrics plus visualization and correlation tools permit users to tailor the protocol to their qualitative and quantitative quality targets.

Nanotechnologies — Measurements of particle size and shape distributions by transmission electron microscopy

1 Scope

This document specifies how to capture, measure and analyse transmission electron microscopy images to obtain particle size and shape distributions in the nanoscale.

This document broadly is applicable to nano-objects as well as to particles with sizes larger than 100 nm. The exact working range of the method depends on the required uncertainty and on the performance of the transmission electron microscope. These elements can be evaluated according to the requirements described in this document.

2 Normative references

The following documents are referred to in the text in such a way that some or all of their content constitutes requirements of this document. For dated references, only the edition cited applies. For undated references, the latest edition of the referenced document (including any amendments) applies.

ISO 9276-3, *Representation of results of particle size analysis — Part 3: Adjustment of an experimental curve to a reference model*

ISO 9276-6:2008, *Representation of results of particle size analysis — Part 6: Descriptive and quantitative representation of particle shape and morphology*

ISO 29301, *Microbeam analysis — Analytical electron microscopy — Methods for calibrating image magnification by using reference materials with periodic structures*

3 Terms, definitions and symbols

For the purposes of this document, the following terms and definitions apply.

ISO and IEC maintain terminological databases for use in standardization at the following addresses:

— ISO Online browsing platform: available at https://www.iso.org/obp

— IEC Electropedia: available at http://www.electropedia.org/

3.1 Core terms — Particles

3.1.1
nano-object
discrete piece of material with one, two or three external dimensions in the *nanoscale* (3.1.2)

[SOURCE: ISO/TS 80004-2:2015, 2.2]

3.1.2
nanoscale
length range approximately from 1 nm to 100 nm

[SOURCE: ISO/TS 80004-1:2015, 2.1, modified — Note 1 to entry has been deleted.]

3.1.3
particle
minute piece of matter with defined physical boundaries

[SOURCE: ISO 26824:2013, 1.1, modified — Notes 1, 2 and 3 to entry have been deleted.]

3.1.4
constituent particle
identifiable, integral component of a larger *particle* (3.1.3)

[SOURCE: ISO/TS 80004-2:2015, 3.3, modified — Note 1 to entry has been deleted.]

3.1.5
agglomerate
collection of weakly or medium strongly bound *particles* (3.1.3) where the resulting external surface area is similar to the sum of the surface areas of the individual components

Note 1 to entry: The forces holding an agglomerate together are weak forces, for example van der Waals forces or simple physical entanglement.

Note 2 to entry: Agglomerates are also termed secondary particles and the original source particles are termed primary particles.

[SOURCE: ISO/TS 80004-2:2015, 3.4]

3.1.6
aggregate
particle (3.1.3) comprising strongly bonded or fused particles where the resulting external surface area may be significantly smaller than the sum of calculated surface areas of the individual components

Note 1 to entry: The forces holding an aggregate together are strong forces (for example, covalent bonds) or those resulting from sintering or complex physical entanglement.

Note 2 to entry: Aggregates are also termed secondary particles and the original source particles are termed primary particles.

Note 3 to entry: Entries 3.1.6 to 3.1.10 define elements of agglomerates and aggregates, some of which are illustrated in Figure 1. Constituent particles in an aggregate are tightly fused into a discrete entity (the aggregate), while the constituent particles in an agglomerate are weakly bound and generally easily dispersed under shear or mechanical stress.

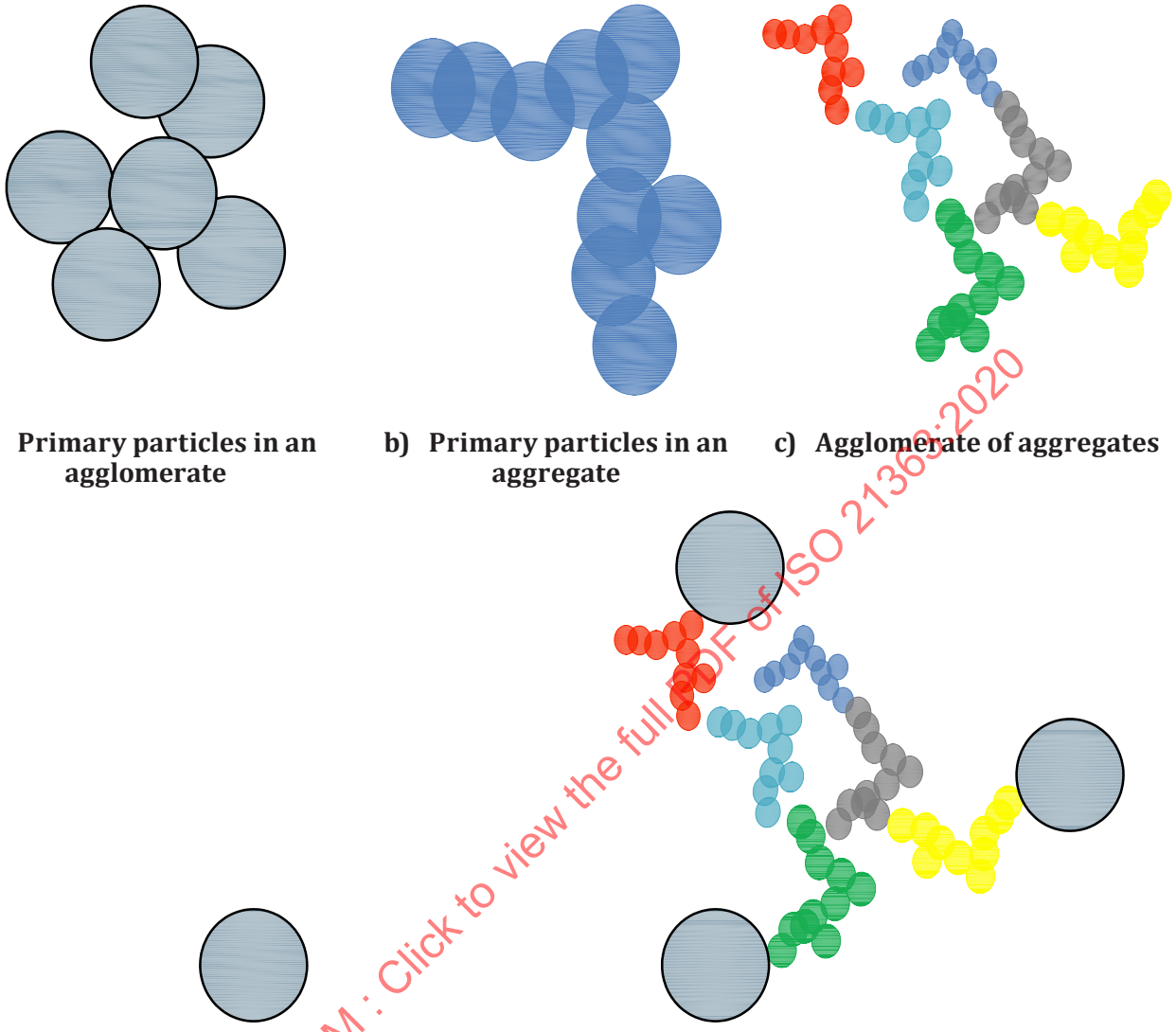

a) Primary particles in an agglomerate

b) Primary particles in an aggregate

c) Agglomerate of aggregates

d) Nano-object (if less than 100 nm) or particle

e) Agglomerate of both primary particles and aggregates

Figure 1 — Schematic showing elements of agglomerates and aggregates

[SOURCE: ISO/TS 80004-2:2015, 3.5, modified — In the definition, "may be significantly smaller" has replaced "is significantly smaller" and "calculated" has been added before "surface areas". In Note 1 to entry, "ionic bonds" in the example and the final phrase "or otherwise combined former primary particles" have been deleted. Note 3 to entry and Figure 1 have been added.]

3.1.7
nanoparticle
nano-object (3.1.1) with all three external dimensions in the *nanoscale* (3.1.2) where the lengths of the longest and shortest axes of the nano-object do not differ significantly

[SOURCE: ISO/TS 80004-2:2015, 4.4, modified — "three" has been added and Note 1 to entry has been deleted.]

3.1.8
nanorod
solid *nanofibre* (3.1.9)

[SOURCE: ISO/TS 80004-2:2015, 4.7]

3.1.9
nanofibre
nano-object (3.1.1) with two similar external dimensions in the *nanoscale* (3.1.2) and the third dimension significantly larger

[SOURCE: ISO/TS 80004-2:2015, 4.5, modified — "similar" has been added and Notes 1, 2 and 3 to entry have been deleted.]

3.1.10
nanophase
physically or chemically distinct region or collective term for physically distinct regions of the same kind in a material with the discrete regions having one, two or three dimensions in the *nanoscale* (3.1.2)

Note 1 to entry: *Nano-objects* (3.1.1) embedded in another phase constitute a nanophase.

3.1.11
nanodispersion
material in which *nano-objects* (3.1.1) or a *nanophase* (3.1.10) are dispersed in a continuous phase of a different composition

[SOURCE: ISO/TS 80004-4:2011, 2.14]

3.1.12
particle size
x
dimension of a *particle* (3.1.3) determined by a specified measurement method and under specified measurement conditions

Note 1 to entry: Different methods of analysis are based on the measurement of different physical properties. Independent of the particle property actually measured, the particle size can be reported as a linear dimension, an area or a volume.

Note 2 to entry: The symbol *x* is used denote linear particle size. However, it is recognized that the symbol *d* is also widely used. Therefore, the symbol *x* may be replaced by *d*.

[SOURCE: ISO 9276-1:1998, 4.2, modified — Converted into a term and definition entry.]

3.1.13
particle size distribution
distribution of *particles* (3.1.3) as a function of *particle size* (3.1.12)

[SOURCE: ISO/TS 80004-6:2013, 3.1.2, modified — Note 1 to entry has been deleted.]

3.1.14
particle shape
external geometric form of a *particle* (3.1.3)

Note 1 to entry: Shape description requires two scalar descriptors, i.e. length and spread.

[SOURCE: ISO/TS 80004-6:2013, 3.1.3, modified — Note 1 to entry has been added.]

3.1.15
particle shape distribution
distribution of a specific *particle shape* (3.1.14) descriptor for a sample population

3.2 Core terms — Image capture and analysis

3.2.1
field of view
field that is viewed by the viewing device

[SOURCE: ISO 13322-1:2014, 3.1.6, modified — Note 1 to entry has been deleted.]

3.2.2
measurement frame
selected area from the *field of view* (3.2.1) in which *particles* (3.1.3) are sized and counted for image analysis

[SOURCE: ISO 13322-1:2014, 3.1.10]

3.2.3
binary image
digitized image consisting of an array of *pixels* (3.2.4), each of which has a value of 0 or 1, whose values are normally represented by dark and bright regions on the display screen or by the use of two distinct colours

[SOURCE: ISO 13322-1:2014, 3.1.2]

3.2.4
pixel
smallest element of an image that can be uniquely processed, and is defined by its spatial coordinates and encoded with colour values

[SOURCE: ISO 12640-2:2004, 3.6, modified — Note 1 to entry has been deleted.]

3.2.5
pixel-resolution
number of imaging *pixels* (3.2.4) per unit distance of the detector

[SOURCE: ISO 29301:2017, 3.24, modified — Note 1 to entry has been deleted.]

3.2.6
pixel count
total number of *pixels* (3.2.4) per file, length, or area depending on the unit used

[SOURCE: ISO 19262:2015, 3.191]

3.2.7
micrograph
record of an image formed by a microscope

[SOURCE: ISO 10934-1:2002, 2.94]

3.2.8
artefact
artifact
unwanted distortion or added feature in measured data arising from lack of idealness of equipment

[SOURCE: ISO 18115-2: 2013, 5.6]

3.3 Core terms — Statistical symbols and definitions

3.3.1
coefficient of variation
C_v
ratio of the standard deviation to the arithmetic mean

Note 1 to entry: It is commonly reported as a percentage.

Note 2 to entry: For example, the coefficient of variation for a sample mean may be represented by:

$$c_v = \frac{s \cdot 100}{\bar{x}}$$

where $\bar{x}$ is the descriptor's mean and s is the descriptor's standard deviation for several datasets. These "grand statistics" are used to evaluate descriptor data for interlaboratory comparisons.

[SOURCE: ISO 27448:2009, 3.11, modified — Notes 1 and 2 to entry have been added.]

3.3.2
standard error of estimation

σ_{est}

measure of dispersion of the dependent variable (output) about the least-squares line obtained by curve fitting or regression analysis

Note 1 to entry: The standard error of estimation may be determined by:

$$\sigma_{est} = \sqrt{\frac{\sum_{i=1}^{n} (y_i - \bar{y})^2}{n-k}}$$

where

- n is the number of data points;
- k is the number of coefficients in the equation.

Note 2 to entry: The standard error of the mean may be determined by:

$$\sigma_{est,\bar{x}} = \frac{s}{\sqrt{n}}$$

Note 3 to entry: The standard error is the standard deviation of the sampling distribution of a statistic. The example is for a sample mean. Standard error of the mean is an estimate of how close the sample mean is to the population mean. This value decreases as the sample size increases.

[SOURCE: ISO 772:2011, 7.31, modified — The admitted term "residual standard deviation" has been deleted. Notes 1, 2 and 3 to entry have replaced the original Notes 1 and 2 to entry.]

3.3.3
relative standard error
RSE

standard error divided by its statistic

Note 1 to entry: It is expressed as a percentage.

Note 2 to entry: For example, the relative standard error of the mean is:

$$RSE_{\bar{x}} = \frac{100 \cdot \sigma_{est,x}}{\bar{x}}$$

3.3.4
measurement bias

estimate of a systematic measurement error

Note 1 to entry: Bias is present when a statistic is systematically different than the population parameter it is estimating.

$\Delta m = |c_m - c_{crm}|$: the absolute difference between the mean measured value and the certified value. Bias of the normal mean of this study would be the average of the individual absolute differences between a measured mean and the certified reference material mean.

$$\text{bias} = \frac{\sum_{i=1}^{n} \Delta_{m,i}}{n}$$

[SOURCE: ISO/IEC Guide 99:2007, 2.18, modified — Notes 1 and 2 to entry have been added.]

3.3.5
residual
difference between the observed value of the response variable and the estimated value of the response variable

3.3.6
residual standard deviation
description of the scatter of the information values about the calculated regression line

Note 1 to entry: It is a figure of merit, describing the *precision* (3.5.5) of the calibration.

[SOURCE: ISO 8466-1:1990, 2.5]

3.3.7
quantile plot
graphical method of comparing two distributions where the quantiles of the empirical (data) distribution are plotted on the y-axis while the quantiles of the theoretical (reference) distribution with the same mean and variance as the empirical distribution are plotted on the x-axis

3.4 Core terms — Measurands

3.4.1
measurand
quantity intended to be measured

[SOURCE: ISO/IEC Guide 99:2007, 2.3, modified — The notes have been deleted.]

3.4.2
image descriptor
descriptor extracted from one image

[SOURCE: ISO/IEC 15938-13:2015, 2.1]

3.4.3
Feret diameter
distance between two parallel tangents on opposite sides of the image of a *particle* (3.1.3)

Note 1 to entry: The *maximum Feret diameter* (3.4.4) is used in this document.

[SOURCE: ISO 13322-1:2014, 3.1.5, modified — Note 1 to entry has been added.]

3.4.4
maximum Feret diameter
maximum length of an object whatever its orientation

[SOURCE: ISO/TR 945-2:2011, 2.1, modified — Note 1 to entry has been deleted.]

3.4.5
minimum Feret diameter
minimum length of an object whatever its orientation

3.4.6
perimeter
total length of the object contour

[SOURCE: ISO/TR 945-2:2011, 2.3]

3.4.7
equivalent circular diameter
diameter of a circle having the same area as the projected image of the *particle* (3.1.3)

EXAMPLE The ecd is:

$$\text{ecd} = \sqrt{\frac{4 \cdot A}{\pi}}$$

where A is the area of the particle.

[SOURCE: ISO 13322-1:2014, 3.1.1, modified — Note 1 to entry has been deleted and the example has been added.]

3.4.8
equivalent perimeter diameter
d_{epd}
diameter of a circle having the same *perimeter* (3.4.6) as the projected image of the *particle* (3.1.3)

Note 1 to entry: It may be calculated as follows:

$$d_{\text{epd}} = \frac{P}{\pi}$$

where P is the length of the perimeter.

3.4.9
convex hull
smallest convex set containing a given geometric object

[SOURCE: ISO 19123:2005, 4.1.2]

3.4.10
aspect ratio
ratio of the *minimum* (3.4.5) to the *maximum Feret diameter* (3.4.4)

Note 1 to entry: It may be calculated, for example, as follows:

$$\text{aspect ratio} = \frac{x_{\text{Fmin}}}{x_{\text{Fmax}}}$$

where

x_{Fmin} is the minimum Feret diameter;

x_{Fmax} is the maximum Feret diameter.

[SOURCE: ISO 26824:2013, 4.5, modified — Note 1 to entry has replaced the original Notes 1 and 2 to entry.]

3.4.11
ellipse ratio
ratio of the lengths of the axes of the Legendre ellipse of inertia

Note 1 to entry: For example, the ellipse ratio can be the ratio of the minor and major axes of the Legendre ellipse fitted to the *particle* (3.1.3); elliptical shape factor, thus:

$$\text{ellipse ratio} = \frac{x_{\text{Lmin}}}{x_{\text{Lmax}}}$$

where

x_{Lmin} is the length of the minor axis of Legendre ellipse of inertia;

x_{Lmax} is the length of the major axis of Legendre ellipse of inertia.

[SOURCE: ISO 26824:2013, 4.4, modified — Note 1 to entry has been replaced.]

3.4.12
extent
bulkiness
ratio of particle area to the product of the *Feret* (3.4.3) and the *minimum Feret diameters* (3.4.6)

Note 1 to entry: For example, the extent may be calculated as:

$$\text{extent} = \frac{A}{x_{Fmin} \cdot x_{Fmax}}$$

where

x_{Fmin} is the minimum Feret diameter;

x_{Fmax} is the maximum Feret diameter.

[SOURCE: ISO 9276-6:2008, 8.1.3, modified — Converted into a term and definition entry. The definition has been added.]

3.4.13
compactness
degree to which the projection area *A* of the *particle* (3.1.3) is similar to a circle, considering the overall form of the *particle* (3.1.3) with the *maximum Feret diameter* (3.4.4)

Note 1 to entry: For example, the compactness may be calculated as:

$$\text{compactness} = \frac{\sqrt{\frac{4 \cdot A}{\pi}}}{X_{Fmax}}$$

where

A is the area of the particle;

x_{Fmax} is the maximum Feret diameter.

[SOURCE: ISO 9276-6:2008, 8.1.3, modified — Converted into a term and definition entry. In the definition, "projection area *A* of the particle" has replaced "particle (or its projection area)" and "with the maximum Feret diameter" has been added.]

3.4.14
convexity
ratio of the *perimeter* (3.4.6) of the *convex hull* (3.4.9) envelope bounding the *particle* (3.1.3) to its perimeter

Note 1 to entry: For example, the convexity may be calculated as:

$$\text{convexity} = \frac{P_C}{P}$$

where

P_c is the length of the perimeter of the convex hull (envelope) bounding the particle;

P is the length of the perimeter.

[SOURCE: ISO 9276-6:2008, 8.2, modified — Converted into a term and definition entry. The definition has been added.]

3.4.15
circularity
C
degree to which the projected area of the *particle* (3.1.3) is similar to a circle, based on its *perimeter* (3.4.6)

Note 1 to entry: For example, the circularity may be calculated as:

$$C = \frac{x_a}{x_p} = \sqrt{\frac{4 \cdot \pi \cdot A}{P^2}}$$

where

x_a is the area-equivalent diameter of a particle;

x_p is the perimeter-equivalent diameter of particle;

A is the area of the particle;

P is the length of the perimeter.

[SOURCE: ISO 26824:2013, 4.12, modified — "projected area of the particle" has replaced "projection area of the particle *A*", "based on its perimeter" has replaced "considering the smoothness of its perimeter *P*". The formula and Note 1 to entry have been replaced.]

3.4.16
roundness
square of the *compactness* (3.4.13)

3.4.17
solidity
ratio of the projected area *A* to the area of the *convex hull* (3.4.9) A_C (envelope)

Note 1 to entry: For example, the solidity may be calculated as:

$$\text{solidity} = \frac{A}{A_C}$$

[SOURCE: ISO 26824:2013, 4.13, modified — Note 1 to entry has been added.]

3.5 Core terms — Metrology

3.5.1
repeatability condition of measurement
condition of measurement, out of a set of conditions that includes the same measurement procedure, same operators, same measuring system, same operating conditions and same location, and replicate measurements on the same or similar objects over a short period of time

[SOURCE: ISO/IEC Guide 99:2007, 2.20, modified — The admitted term "repeatability condition" and the notes have been deleted.]

3.5.2
intermediate precision condition of measurement
condition of measurement, out of a set of conditions that includes the same measurement procedure, same location, and replicate measurements on the same or similar objects over an extended period of time, but may include other conditions involving changes

[SOURCE: ISO/IEC Guide 99:2007, 2.22, modified — The admitted term "intermediate precision condition" and the notes have been deleted.]

3.5.3
reproducibility condition of measurement
condition of measurement, out of a set of conditions that includes different locations, operators, measuring systems, and replicate measurements on the same or similar objects

Note 1 to entry: The different measuring systems may use different measurement procedures.

Note 2 to entry: A specification should give the conditions changed and unchanged, to the extent practical.

[SOURCE: ISO/IEC Guide 99:2007, 2.24, modified — The admitted term "reproducibility condition" has been deleted.]

3.5.4
measurement accuracy
closeness of agreement between a measured quantity value and a true quantity value of a *measurand* (3.4.1)

Note 1 to entry: The concept "measurement accuracy" is not a quantity and is not given a numerical quantity value. A measurement is said to be more accurate when it offers a smaller measurement uncertainty.

Note 2 to entry: The term "measurement accuracy" should not be used for measurement trueness and the term "measurement precision" should not be used for "measurement accuracy", which, however, is related to both these concepts.

Note 3 to entry: "Measurement accuracy" is sometimes understood as closeness of agreement between measured quantity values that are being attributed to the measurand.

[SOURCE: ISO/IEC Guide 99:2007, 2.13, modified — The admitted terms "accuracy of measurement" and "accuracy" have been deleted. In Note 1 to entry, "measurement uncertainty" has replaced measurement error".]

3.5.5
precision
measurement precision
closeness of agreement between indications or measured quantity values obtained by replicate measurements on the same or similar objects under specified conditions

Note 1 to entry: Measurement precision is usually expressed numerically by measures of imprecision, such as standard deviation, variance, or *coefficient of variation* (3.3.1) under the specified conditions of measurement.

Note 2 to entry: The "specified conditions" can be, for example, *repeatability conditions of measurement* (3.5.1), *intermediate precision conditions of measurement* (3.5.2), or *reproducibility conditions of measurement* (3.5.3) (see ISO 5725-3:1994).

Note 3 to entry: Measurement precision is used to define measurement repeatability, intermediate measurement precision, and measurement reproducibility.

Note 4 to entry: Sometimes "measurement precision" is erroneously used to mean *measurement accuracy* (3.5.4).

[SOURCE: ISO/IEC Guide 99:2007, 2.15, modified — "precision" has been made the preferred term and "measurement precision" the admitted term.]

3.5.6
combined standard measurement uncertainty
standard measurement uncertainty that is obtained using the individual standard measurement uncertainties associated with the input quantities in a measurement model

Note 1 to entry: In cases of correlations of input quantities in a measurement model, covariances shall be taken into account when calculating the combined standard measurement uncertainty; see also ISO/IEC Guide 98-3:2008, 2.3.4.

3.5.7
expanded measurement uncertainty
U
product of a *combined standard measurement uncertainty* (3.5.6) and a factor larger than the number one

Note 1 to entry: The factor depends upon the type of probability distribution of the output quantity in a measurement model and on the selected coverage probability.

Note 2 to entry: The term "factor" in this definition refers to a coverage factor.

Note 3 to entry: Expanded measurement uncertainty is termed "overall uncertainty" in paragraph 5 of Recommendation INC-1 (1980) (see the GUM) and simply "uncertainty" in IEC documents.

[SOURCE: ISO/IEC Guide 99:2007, 2.35, modified — The admitted term "expanded uncertainty" has been deleted. The symbol "*U*" has been added.]

3.5.8
Type A evaluation of measurement uncertainty
evaluation of a component of measurement uncertainty by a statistical analysis of measured quantity values obtained under defined measurement conditions

[SOURCE: ISO/IEC Guide 99:2007, 2.28, modified — The admitted term "Type A evaluation" and the notes have been deleted.]

3.5.9
Type B evaluation of measurement uncertainty
evaluation of a component of measurement uncertainty determined by means other than a *Type A evaluation of measurement uncertainty* (3.5.8)

[SOURCE: ISO/IEC Guide 99:2007, 2.29, modified — The admitted term "Type B evaluation", the note and the examples have been deleted.]

3.5.10
reference material
RM
material, sufficiently homogeneous and stable with respect to one or more specified properties, which has been established to be fit for its intended use in a measurement process

[SOURCE: ISO Guide 30:2015, 2.1.1, modified — The notes to entry have been deleted.]

3.5.11
certified reference material
CRM
reference material (RM) (3.5.10) characterized by a metrologically valid procedure for one or more specified properties, accompanied by an RM certificate that provides the value of the specified property, its associated uncertainty, and a statement of metrological traceability

[SOURCE: ISO Guide 30:2015, 2.1.2, modified — The notes to entry have been deleted.]

3.6 Core terms — Transmission electron microscopy

3.6.1
transmission electron microscopy
TEM
method that produces magnified images or diffraction patterns of the sample by an electron beam, which passes through the sample and interacts with it

[SOURCE: ISO/TS 80004-6:2013, 3.5.6]

3.6.2
scanning transmission electron microscopy
STEM
method that produces magnified images or diffraction patterns of the sample by a finely focused electron beam, scanned over the surface and which passes through the sample and interacts with it

[SOURCE: ISO/TS 80004-6:2013, 3.5.7, modified — The notes to entry have been deleted.]

3.6.3
accelerating voltage
potential difference applied between the filament and anode in order to accelerate the electrons emitted from the source

[SOURCE: ISO 22309:2011, 3.3, modified — Note 1 to entry has been deleted.]

3.6.4
bright-field transmission electron microscopy
bright-field TEM
TEM technique of electron illumination and imaging in which the direct electron beam passes through the sample and the image is formed only by the transmitted wave, by selecting the wave using an objective aperture on the back focal plane

Note 1 to entry: Generally, the portions of the sample that are thicker or that have a higher atomic number (Z) appear darker against a brighter background. In this mode, the contrast, when considered classically, is formed directly by occlusion and absorption of electrons in the sample. Thicker regions of the sample, or regions with a higher atomic number, will appear dark, while regions with no sample in the beam path will appear bright, hence the term “bright-field”.

Note 2 to entry: This will be included in a vocabulary on analytical electron microscopy, which is under preparation by ISO/TC 202/SC 1.

[SOURCE: ISO/TS 10797:2012, 3.3]

3.6.5
dark-field transmission electron microscopy
dark-field TEM
TEM technique of electron illumination and imaging in which the direct electron beam passes through the sample and the image is formed only by diffracted wave, by selecting the wave using an objective aperture on the back focal plane

Note 1 to entry: Crystalline parts of the sample disperse the electrons of the direct beam into discrete locations in the back focal plane. By the placement of apertures in the back focal plane, i.e. the objective aperture, desired portions of the reflections can be selected, thus only those parts of the sample that are causing the electrons to scatter to the selected reflections will be imaged. If the selected reflections do not include the unscattered beam, then the image will appear dark wherever no sample scattering to the selected peak is present – hence the term “dark-field”.

Note 2 to entry: Modern TEMs are often equipped with sample holders that allow the user to tilt the sample to obtain specific diffraction conditions. The wave that caused scattering and reflection (for example, Bragg reflection) in a crystalline sample will form a dark-field image by selecting a specific diffraction wave through objective apertures placed on the back focal plane of objective lens.

Note 3 to entry: High-angle annular dark-field imaging (HAADF) is highly sensitive to variations in the atomic number of atoms in the sample and produces so-called *Z*-contrast images, which yield useful information on the presence of metals on nanotubes and catalyst residues, even when these small metal *particles* (3.1.3) are imbedded within amorphous carbon or catalyst support while otherwise invisible in bright-field imaging mode.

Note 4 to entry: This will be included in a vocabulary on analytical electron microscopy, which is under preparation by ISO/TC 202/SC 1.

[SOURCE: ISO/TS 10797:2012, 3.4]

3.7 Statistical symbols, measurands and descriptors

3.7.1 Statistical symbols

C_v coefficient of variation

$q(x)$ differential distribution (density distribution)

$Q(x)$ cumulative distribution

p statistic returned from analysis of variance or bivariate analysis

RSE relative standard error

s standard deviation of the descriptor, x, or the descriptor parameter

s^2 variance of the descriptor or the descriptor parameter

σ_{est} standard error of estimation

x value of the descriptor or descriptor parameter

$\bar{x}$ mean of the descriptor or descriptor parameter

$X(x)$ transform of the descriptor (e.g. $X(x) = x$ for a normal distribution, $X(x) = \ln x$ for a lognormal distribution)

$Y(Q)$ transform of Q plotted on the y-axis, i.e. Y = inverse of the distribution. Other transforms are listed in ISO 9276-3:2008, Table 1.

NOTE Quantity measures and types of distributions are defined in ISO 9276-1:1998.

3.7.2 Measurands and descriptors

NOTE Measurands or descriptors for size and shape measurements can be directly proportional to length (Category 1) or proportional to length squared (Category 2).

3.7.2.1 Size descriptors and symbols — Category 1

P length of the perimeter

P_c length of the perimeter of the convex hull (envelope) bounding the particle

x_a area-equivalent diameter of a particle [also known as “equivalent circle diameter (ECD)”]

x_{Fmax} maximum Feret diameter; corresponds to the “length” of the particle

x_{Fmin} minimum Feret diameter; corresponds to the “breadth” of the particle

x_{Lmax} length of the major axis of Legendre ellipse of inertia,

x_{Lmin} length of the minor axis of Legendre ellipse of inertia

x_p perimeter-equivalent diameter of particle

$$x_p = \frac{P}{\pi}$$

3.7.2.2 Size descriptors and symbols — Category 2

A area of the particle

A_c area of the convex hull (envelope) bounding the particle

L^2 area computed by the multiplication of two lengths

NOTE Volume-equivalent diameter, x_V, and surface-equivalent diameter, x_S, are not included as they are three-dimensional descriptors.

3.7.2.3 Shape descriptor symbols — Category 1

AR aspect ratio

ER ellipse ratio

NOTE 1 ISO elongation shape descriptors for image analysis are defined such that their values scale from zero to one, rather than the inverse definition, which is quite common throughout the rest of the literature. The ISO definitions limit the descriptor variable range, making probability and cumulative density plots more compact.

C circularity

NOTE 2 ISO elongation shape descriptors for image analysis are defined such that their values scale from zero to one, rather than the inverse definition, which is quite common throughout the rest of the literature. The ISO definitions limit the descriptor variable range, making probability and cumulative density plots more compact.

4 Stakeholder needs for TEM measurement procedures

This document addresses the following needs of the user community for size and shape distributions:

a) commercially available materials should be measured;

b) the capture, measurement and analysis of the data should be automated as much as practical;

c) workflows should facilitate decisions about image capture, particle measurement and data analysis;

d) case study examples should illustrate:

   1) the identification of touching particles, unselected particles and artefacts;

   2) the selection of size and shape descriptors with high repeatability and reproducibility;

   3) the estimation of measurement uncertainties for distribution parameters, i.e. mean and spread;

   4) the differentiation between samples using size and shape descriptors;

   5) the use of data visualization tools to augment measurement uncertainty results.

Figure 2 illustrates the workflow for the measurement of particle size and shape distributions that addresses stakeholder needs. It is important to identify any particles that are not targets of the investigation. It may also be necessary or preferred to remove touching particles. Data repeatability, intermediate precision or reproducibility should be quantitated, depending on the application. Fitting distributions to data provides values for the mean and spread of reference distributions, for which measurement uncertainties can be estimated. In some cases, the individual numerical results (mean, spread and their uncertainties) alone cannot differentiate between models and/or data. Visualization tools and correlations can provide additional information about the test sample.

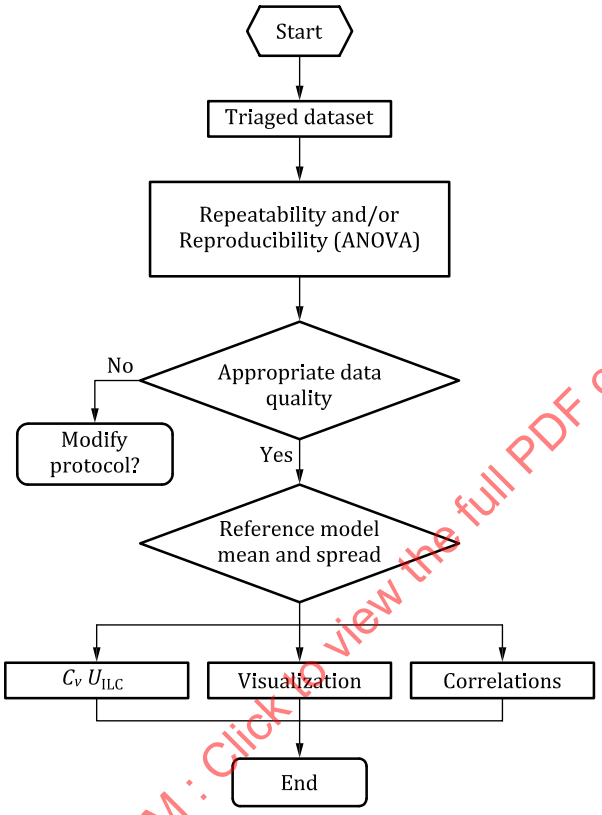

Figure 2 — Workflow for measurement of particle size and shape distributions by TEM

5 Sample preparation

5.1 General

The procedural steps (sample preparation, instrument set-up and calibration and image capture) are highly interdependent. All contribute to generating high quality datasets of size and shape descriptors. Statistical tools, such as analysis of variance, fitting distribution models to the data and bivariate analysis, can help the researcher tune the entire procedure to provide the accuracy or measurement uncertainty needed for the specific sample.

Often, a large number of nanoparticles will need to be imaged and analysed to obtain a particle size distribution. Particle analysis time can be reduced and data quality can be improved when image analysis software is used. When procedures are developed for unknown samples, it can be useful to go through the entire process to determine which factors are critical for the sample at hand. Analysis will be facilitated when image analysis software is used. Both commercial and open source software are available. The images shall be of sufficient quality such that individual particles can be resolved and their dimensions measured. An important objective of sample preparation is to generate uniform distributions of particles across mounting substrates.

5.2 Sample sources

Samples will typically be supplied as powders or suspensions. Powder samples are often dispersed in liquids prior to their deposition on a substrate for TEM evaluation. Suspensions often need to be diluted in order to image discrete particles. Key sample preparation objectives are:

— use a representative sample of the powder or liquid;

— minimize agglomeration in the dispersion used for mounting the sample;

— minimize particle-particle associations on the support;

— distribute the sample uniformly across the support (see ISO 9276-3);

— select a support that enhances the contrast between particle and background.

Health effect information of various nanoparticles is still being assembled. It is likely that some nanoparticles are hazardous to health while others may not be hazardous or may not cause adverse health effects following exposure. Sample preparation should be done wearing appropriate personal protective equipment, including disposable gloves, safety glasses, laboratory coats, filter respirators, etc. Sample preparation should be carried out in a vented fume hood equipped with suitable air filters.

5.3 Use a representative sample

5.3.1 General

During manufacturing processes for engineered nanomaterials, the nanoparticles may exist in several colloidal states. For example, chemical vapour deposition or physical vapour deposition processes can generate “seeds” that can become nanoparticle aerosols. Rapidly cooling liquid nanoparticles can solidify, fusing together at their surfaces prior to solidification, yielding aggregated products that have dimensions greater than one micrometre but originate from many particles. Since the original primary particles are often not recognizable in the aggregate, the term “constituent particle” is used to describe the particles that can be discerned inside an aggregate.

5.3.2 Powder samples

Powder samples need to be taken carefully, as material can redistribute under the vibrations and forces of transportation. The samples also need to be handled carefully, particularly if they are aggregated and can fracture with mechanical action. ISO 14887:2000 and ISO 14488:2007 provide guidance on how to take and handle powder samples. Most powders and nanoparticles will be negatively charged in the gas phase, so loading dry samples on substrate surfaces, which are also usually negatively charged, often results in large agglomerates that are difficult to image. Powder samples are usually prepared for TEM imaging by dispersing them in a liquid phase, which is then deposited on the measurement substrate or grid.

5.3.3 Nanoparticle dispersions in liquids

In other manufacturing systems, the nanoparticle precursors are dispersed to colloidal dimensions first in a liquid phase, followed by conversion to liquid sols. Stable colloidal dispersions in the liquid phase usually require either electrostatic or steric stabilization methods in order to prevent agglomeration. Concentrated nanoparticle dispersions shall be diluted in order to reduce touching nanoparticles on the measurement substrate or grid. The stability of colloidal dispersions affects whether they remain as discrete particles or agglomerate, aggregate or flocculate. Colloid stability depends on the particle surface chemistry, coatings or adducts on the particles, solvent chemistry, and inorganic and organic ligands in the fluid phase. Sonication can be effective in dispersing some nanoparticles in liquids, as shown in the some of the case studies.

5.4 Minimize particle agglomeration in the sample dispersion

Forces that affect the stability of colloidal systems include:

— excluded volume repulsion;

— electrostatic interaction;

— van der Waals forces;

— entropic forces ;

— steric interactions.

Mutual repulsion of like electrical charges on nanoparticle colloids leads to electrostatic stabilization. Electrical double layers can form at the nanoparticle/liquid interface. Due to their small size, nanoparticles can have very large surface areas per volume (mass), so repulsive surface forces can overcome buoyancy forces that might lead to particulate settling. Steric stabilization of colloids occurs when coatings, such as polymers or oligomers, are attached to the nanoparticle surfaces. These coatings prevent the nanoparticles from approaching close enough that attractive forces would become effective, thus preventing agglomeration.

Many commercial nanoparticle products have surface coatings or surface functionalizations that are designed to control their dispersion in specific media. Destabilization of nanoparticle colloids in liquid dispersions can occur via a variety of mechanisms. The common methods for controlling the interactive forces between particles are selection of the dispersing liquid and the dispersing agent (see ISO 14887 and Reference [22]). Selection of the dispersing liquid is usually preferred if the chosen liquid reduces or prevents particle agglomeration, as dispersing agents coat the nanoparticles. Depending on the size ratio between the nanoparticle and the dispersing agent, the agent may affect the imaging of particle surfaces and cross-sections. Also, dispersing aids can desorb from the nanoparticles or may induce nanoparticle agglomeration with changes in temperature and liquid phase composition; they shall be chosen with care.

5.5 Selection of the mounting support

Several common methods for depositing nanoparticles on measurement substrates are available (see Reference [22]). A preferred support has most of the following characteristics:

— flat over the field of view selected;

— uniform and low background intensity (bright field) across the field of view;

— good contrast between particles and background.

Different types of samples often require different specimen preparation strategies, i.e. other commonly applied standards are based on grid-on-drop and on-grid centrifugation. Particle composition, particle surface chemistry, dispersing solvent, acidic or basic conditions, mounting support modifications and other factors contribute to the quality of the mounting support and mounting technique. Therefore, specimen preparation, including all consumables and chemicals, shall be described in great detail in the analysis report.

6 Instrument factors

6.1 Instrument set-up

ISO 29301:2017, 6.3, provides guidance on the operating conditions for electron microscopes. The TEM instrument parameters shall be selected[22] to provide high quality images with good contrast between background and particle. To contribute to the TEM image contrast, the nanoparticles shall scatter electrons, which depend on the sample composition and crystalline phase orientation.

6.2 Calibration

6.2.1 General

ISO 13322-1:2014, Clause 10, has generic recommendations on calibration and metrological traceability.

6.2.2 Calibration standards

Since TEMs have a wide range of magnification and many operating modes, the actual magnification at any set of instrument settings may differ from the indicated magnification by up to 10 %. Calibration of the instrument to the SI unit of length (the metre) at optical conditions similar to those used for analysis is preferred. Calibrants shall fulfil all the requirements of a certified reference material (CRM), i.e. they shall be homogenous and stable, come with (a) certified value(s) and associated uncertainty and metrological traceability statement, come with a material certificate, etc. Standards should be run periodically to provide verification of correct instrument operation within manufacturer specifications and to validate measurement procedures. Typical examples are shown in Table 1. Be sure that the standard sample used has not passed its expiration date.

Table 1 — Typical calibration standards

Standard size nm	Material
2 160 lines/mm	Gratings; linear or cross-grating
2 to 100	Polystyrene, gold and silica nanoparticles
> 10	Crystals of catalase enzyme (bovine liver catalase crystals have lattice spacings of 8,75 nm and 6,85 nm[23])

When selecting a calibration technique for a TEM particle size analysis procedure, preference should be given to particle-based CRMs rather than the more traditional line-width standards. For example, calibration against a lattice spacing may only be useful at a magnification that is used to image the particles. These magnifications may not be appropriate for a number of nanoparticles. The calibration validity should be checked on a regular basis. Such quality control should be done with standards/CRMs that are different than the one used for calibration. Furthermore, the verification checks, as well as the (routine) particle size analyses shall be done under similar conditions (in terms of magnification, probe current, acceleration voltage, etc.) as used during calibration.

6.2.3 General calibration procedure

As the calibration strongly depends on the electron optics condition, it shall be done under optimum lens conditions using a suitable CRM. Then, the actual particle size measurement should be done under the same conditions of the calibration with a reference material (RM), e.g. objective lens current and the other lens parameters and specimen height.

The objective lens shall be calibrated to the eucentric axis. The specimen shall be set to the eucentric position using Z-axis movement. The “wobbler” functions can be used as the focus aid. When the sample is positioned on the eucentric axis, the image at the first image plane will have the minimum error in its length (see Figure 3). While the sample is positioned on the eucentric axis, tilting the sample around this axis is the same of tilting on first image plane, so the sample image doesn’t move on the fluorescent screen. If the sample position is not at the eucentric axis, there will be errors in its measured dimensions. Both RM calibrations and sample measurements shall be done with the specimens positioned on the eucentric axis.

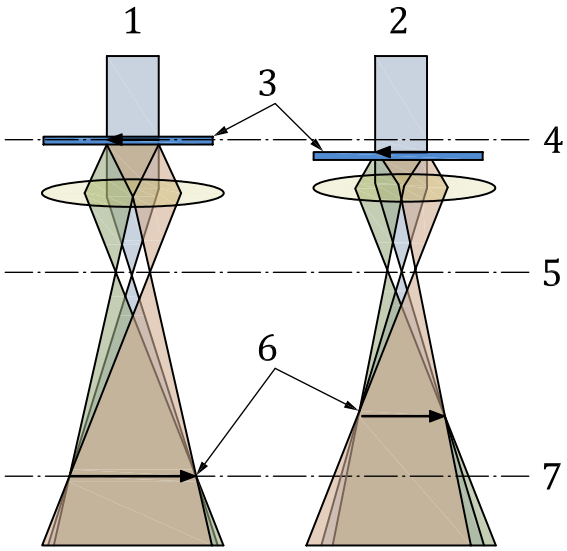

Key

1	on axis	5	back focal plane
2	off axis	6	image
3	specimen	7	first image plane
4	eucentric axis		

NOTE Left hand side: proper alignment. Right hand side: sample displaced from the eucentric axis.

Figure 3 — Example of scale size error due to the specimen plane not coinciding with eucentric axis

TEM projection lenses need to be switched to make accurate measurements across the entire size range of a particle distribution. The lens ranges will depend on the TEM model, for example, low magnification < 100 000 times and high magnification ≥ 100 000 times. In each range, linearity of scaling will be achieved. However, there are discontinuities between calibration lines for different lenses: scale calibration needs to be done for each projection lens used to acquire images. Figure 4 demonstrates such differences in scaling calibration lines for the case of three projection lens systems. Calibration equations change between each lens system resulting in discontinuities (offsets) between the lines for different lenses. Details of scale calibration are provided in ISO 29301.

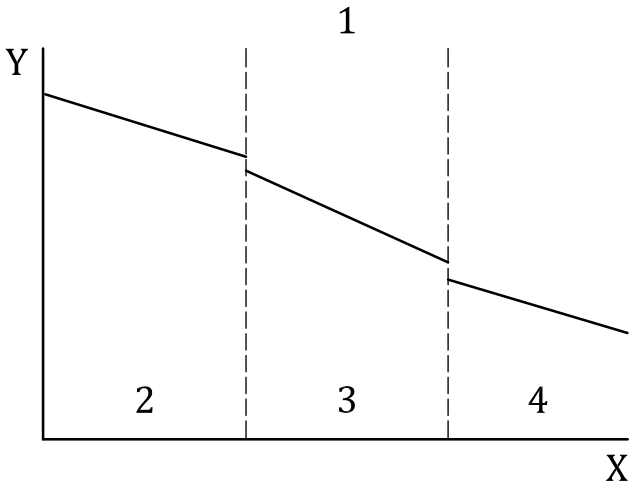

Key

1	projection lens system	X	magnification
2	low magnification	Y	scale/pixel
3	middle magnification		
4	high magnification		

Figure 4 — Linear scaling between magnification and scale/pixel size for different projection lens systems

6.3 Setting TEM operating conditions for calibration

Use the procedure of ISO 29301 to ensure, as far as possible, the same TEM operating conditions.

a) The vacuum in the TEM column should be lower than 10^{-4} Pa and stable.

b) Apply high voltage and allow it to stabilize.

NOTE 1 Oil-filled 100 kV tanks take about 2,5 h. Gas-filled tanks take about 45 min. Higher voltage instruments are normally operated with the high voltage continually applied, therefore a stabilization period is not usually required.

c) Use an anti-contamination device, if needed.

d) Select a specimen region of interest (ROI) for the calibration that is clean and free from damage. Ensure the eucentric height of the ROI and adjust the height of the ROI, if necessary.

e) In order to minimize the effect of the magnetic hysteresis of the lenses, set the magnification of the TEM to the target value for calibration according to the same sequence. For example, adjust higher magnification than the target magnification at first, then set the target magnification after that.

f) Set the excitation of the objective lens to the desired reproducible value. The standard condition is recommended.

g) Adjust the specimen height to focus the magnified image projected on the fluorescent screen, the TV monitor or the personal computer (PC) screen.

NOTE 2 If the TEM in question is not equipped with a specimen-height control function, this procedure can be omitted.

h) Correct astigmatism at a slightly higher magnification than the target value and adjust the accelerating voltage centre. For example, if the target calibration is × 100k, set the magnification in the range, 150k × to 200k × for alignment.

i) Switch the observation mode of the TEM to the selected-area electron-diffraction (SAED) mode or the convergent-beam electron-diffraction (CBED) mode from the image mode. Also, make sure that the objective aperture is removed.

NOTE 3 For the SAED mode, it is necessary to insert a selected-area aperture over the area of interest of the specimen in order to project a SAED pattern on the viewing device (fluorescent screen/TV monitor/PC screen).

j) Adjust the condenser lens system to provide nearly parallel illumination conditions.

k) Align a low-index zone axis of the crystal parallel to the optical axis, i.e. zone-axis illumination, if the specimen is a single crystal.

NOTE 4 This procedure is for a high resolution observation of a specimen. For the size or shape measurement of nanoparticles, this procedure can be omitted.

l) Insert the objective aperture, centring it about the electron optical axis. Also, switch the observation mode of the TEM back to the image mode.

m) Return the magnification to the target value of calibration and set the excitation current of the objective lens to the standard exciting condition again.

n) Apply a relaxation function to relax the magnetic hysteresis of the objective lens, if the TEM has it.

o) Adjust the specimen height to focus the magnified image roughly.

NOTE 5 If the TEM in question is not equipped with a specimen-height control function, this procedure can be omitted.

p) Adjust the fine focus by varying the exciting current of the objective lens.

NOTE 6 If necessary, the Image Wobbler function can be used to focus images.

q) Turn off the auto-focus correction function to the optimum under-focus condition linked with the Image Wobbler function, if the TEM is equipped with this function.

r) Adjust the illumination condition of the condenser lens system (spot size and brightness) with reference to the dynamic range of each detector to obtain image contrast in the whole dynamic range. The condenser lens system should be operated under conditions that approach parallel illumination. Alternatively, it should be operated under a condition where beam convergence no longer affects the image focus. Recording multiple images under varying degrees of beam convergence can help find such a condition.

7 Image capture

7.1 General

Distributions generated from TEM images will be count- or number-based. Much prior work has focused on the number of particles to analyse for the determination of the mean (or average) particle size based on normal size distributions. Theoretically, and in the absence of systematic errors and bias, the uncertainty associated with the mean value of particle size is inversely proportional to the square root of the number of particles analysed. ISO 13322-1:2014, Annex A, provides a measurement uncertainty analysis specifically for lognormal distributions, which would be a common model for size descriptors of nanoparticle systems. Other standards and guidelines[22] also address uncertainty analysis.

7.2 Setting a suitable operating magnification

TEM magnification should be set by considering the range of particle sizes to be analysed and the image capture software to be used for analysis[24]. The field of view should be large enough to include the largest particles while having sufficient resolution to distinguish the smallest particles from

noise. Consider a square-shaped particle has a length dimension of 10 nm and an area of 100 nm^2 for which the resolution is 0,5 nm/pixel. A one-pixel difference in measuring the length dimension of the particle would give a 5 % error in a diameter. A 4-pixel difference in measuring the area would give a 1 % difference in the particle area. The ASTM standard for carbon black[24] provides a starting point for setting the operating magnification. Table 2 shows the uncertainty in a diameter measurement, as a per cent, for a one-pixel difference in reporting a particle length. Note that length measurement errors can occur during image capture or particle analysis. Operators can determine the operating magnification to achieve the needed measurement uncertainty for a descriptor by using the steps provided in this document.

Table 2 — Suggested starting points for setting instrument magnification for different sized nanoparticles[24]

Particle size range nm		**Resolution** nm/pixel		**Uncertainty in diameter measurement for 1 pixel difference in image** %	
Low	High	Low	High	Low	High
14	21	1,5	2,0	11	10
22	26	2,0	2,5	9	10
27	37	2,5	3,0	9	8
38	49	3,0	4,0	8	8
50	62	4,0	5,0	8	8
63	100	5,0	6,0	8	6
101	199	6,0	12,0	6	6
200	400	12,0	20,0	6	5

7.3 Minimum particle area

To reduce pixel count differences of a circle to less than 5 %, the necessary pixel numbers per particle shall range from 100 to 200 in accordance with ISO 9276-6. At a specific magnification level, the number of pixels per nanometer can be estimated, which allows estimates of the number of pixels per square nanometer. Thus, it is often possible to determine, during image capture, whether the uncertainty on smaller particles is acceptable and adjust the magnification if needed. If the particle size distribution is broad, it may be necessary to adjust the resolution to provide accuracy for small particles. In some cases, it may be necessary to take images at two different magnifications to generate data with good size accuracies for large and small particles.

7.4 Number of particles to count for particle size and shape distributions

A major factor affecting the measurement uncertainty of particle size distributions is the number of particles that need to be imaged and measured to improve the degree of confidence in distribution data, and any distribution model fitted to the data. When there is no prior experience with a particular sample, this document suggests a target of acquiring descriptor values for 500 particles in the first dataset. This heuristic was used for some of the case studies reported in the annexes.

NOTE The statistical error between mean descriptor values of the population and of the sample has been analysed by Masuda and Gotoh for lognormal particle diameter distributions[25]. The number of analysed particles required depends in the standard deviation of the sample's descriptor, whether the descriptor distribution is count- or mass-based, the relative error of the descriptor for the desired applications, and what probability level would be acceptable for the descriptor mean based on the selected relative error. The first dataset can then be analysed using the method of Masuda and Gotoh (see Equation 20 and/or Figure 6 of Reference [25]) or by determining the measurement uncertainty using 9.5. The sizes of subsequent datasets could be based on the needed measurement uncertainties or needed probability level for the selected relative error of the descriptor mean.

7.5 Uniform background

Images should be acquired where the frame background is uniform in intensity, and there is good contrast between the particles and the background. It may be necessary to perform the image capture protocol on a few frames prior to analysing all the particles.

The following guidelines should be considered:

— select operating conditions to minimize drift;

— collect images at an appropriate accelerating voltage, e.g. 120 kV;

— set the ratio of the image resolution to the average particle diameter to control measurement uncertainty;

EXAMPLE For a nominal particle diameter of 30 nm measured at a resolution of 0,5 nm/pixel, each pixel would contribute 1,6 % to a particle diameter of the mean size. Smaller particles would have larger sensitivities to measurement uncertainties.

— ensure reproducible calibration settings by performing lens normalization (intended to minimize hysteresis) at the selected magnification for imaging;

— ensure that a scale bar is visible in each digital image;

— do not exclude irregularly shaped particles or particles with sharp corners;

— decide whether or not to reject touching particles;

— reject all particles that appear cut by the frame from the measurement;

— count and report at least 500 particles in frames that are well-spaced across the grid surface;

— report particle size information for all selected particles in each frame.

While many image analysis software programs include methods for separating touching particles, there can be changes in the size and shape distributions when they are used. When such an algorithm was used for size distributions of gold nanospheres[26], the reported mean of the equivalent circular diameter (ECD) distribution decreased, and the reported spread of this distribution decreased. On the other hand, systematic removal of all touching particles may also lead to a non-representative selection of counted particles.

The effects of sample size on the measurement uncertainty of mean particle diameter have been well-studied[25][27][28][29][30], with larger numbers of particles resulting in lower measurement uncertainties. Measurement uncertainty for the distribution parameters, sample mean and standard deviation should also be lower for larger number of particles. The suggested minimum number of particles for analysis of size and shape distributions is 500, based on the experience from prior studies.

There are two options for image analysis: performing individual particle analysis (e.g. particle outlining) or automated image analysis. Automated image analysis is generally preferred when it is possible. Individual particle analysis is described in ISO 13322-1 and is used in Annexes F, G and H.

7.6 Measurement procedure

7.6.1 General

The analysis should be representative of the sample. In general, it is recommended that each sample is analysed in triplicate. Statistical analysis of the data should demonstrate whether the samples are truly representative of the whole[31]. TEM records projected images of particles: particle composition, internal structure and surface morphology may all contribute to the image appearance.

7.6.2 Developing a test sample

A test sample is a portion taken directly from a laboratory sample (material received directly from the applicant) or a sub-sample (representative portion taken from the laboratory sample and transferred to a new vial without sample preparation). The test sample goes through a sample preparation process to generate a test specimen, which is the test sample mounted on a TEM grid. Sample preparation steps can include separations, such as filtration or centrifugation, dispersions in liquids using mechanical energy, such as sonication, and solvent removal, such as drying. All of these steps can affect the morphology of the particles on the TEM grid. While the data analysis techniques of this document have been demonstrated on measurement uncertainty of size and shape descriptors for specified sample preparation protocols, they can also be used to develop protocols that minimize measurement uncertainty for specific samples.

7.6.3 Effects of magnification

A well-aligned, stable TEM should be operated at a magnification that allows many particles to be visible in the field of view and ensures that each particle is recorded with a large number of pixels. For example, nanoparticle samples with d_{ave} = 50 nm, imaged at a magnification of ≈50,000 and recorded on a CCD camera with pixel dimensions (square matrix) of 14 µm, would have a diameter of about 180 pixels. A CCD camera with 2 048 × 2 048 pixels would contain about 120 particles within the field of view of a single micrograph[31].

7.6.4 Frames (micrographs)

Record enough micrographs to image a minimum of 500 particles per sample from a minimum of two widely separated regions of the grid. Image recording times should be sufficiently long so that the ratio of the difference of average grey level between particles and background to the noise level, i.e. the standard deviation of grey level, of the background is at least 5:1. Recording times also should be kept short (1 s to 2 s) to minimize contributions from stage drift[31]. Drift observed during image capture is usually caused by the combined effect of stage and beam drift.

7.7 Revision of image capture protocols

It can be useful to revisit image capture protocols and particle analysis protocols (see Clause 8) after the initial work on data analysis, i.e. raw data triage (see 9.1). Raw data triage is particularly useful when a sample is being analysed for the first time by a given laboratory. All the case studies reported in the annexes went through raw data triage to identify protocol steps that reduced the measurement uncertainties of fitted parameters and improved understanding of the descriptor distributions that represented particle morphologies.

8 Particle analysis

8.1 General

Since a large number of particles are needed for a high-quality particle size distribution, the work will be facilitated when automated image analysis software is used. Both commercial and open source software are available.

8.2 Individual particle analysis

ISO 13322-1 provides guidance on counting procedures, particle edges, particles cut by the edge of the measurement frame, touching particles, measurements, calibration and traceability, and distortion for individual (manual) particle analysis.

8.3 Automated particle analysis

Most of the data reported in the case studies have been analysed using ImageJ, which is freeware from the National Institutes of Health (NIH)[32][33]. A number of commercial software packages are also available. A first objective for measuring particle size distributions is to transform the digital micrograph from a grey-scale image into a binary image consisting of discrete particles and background. Each pixel value shall be classified by thresholding the image and tabulating the number pixels for each particle. Imaging threshold operations are subject to user bias and automation is preferred. When the background values are not uniform across the image, automated methods may fail. The user would need to manually select threshold values for different regions of the image[31].

After thresholding is completed, particles can be identified. A particle will consist of a large number of contiguous pixels that meet the thresholding criteria. There may be some background pixels with binary values that exceed the thresholding criteria. These will usually be singular or small numbers of pixels, which should be eliminated from analysis. In ImageJ, there are "despeckle", "erode" and "dilate" functions. Applying this combination of steps usually removes artefacts created by the software acting on the pixels. A visual comparison of the original image and the treated image should confirm that appropriate artefacts were removed. Similarly, there may be some pixels within the nanoparticle set that are below the threshold limit. These holes would be "filled" by the software to permit analysis. Some specific examples on automated analysis are provided by the collaboration of the National Institute of Standards and Technology with the Nanotechnology Characterization Laboratory (NIST-NCL) (PCC-15[34]), the National Institute of Occupational Safety and Health in collaboration with Dune Scientific (NIOSH/DUNE, see pp. 5–10 of Reference [35]), and a Good Practice Guide from the National Physical Laboratory (see pp. 36–40 of Reference [22]).

8.4 Example — Automated particle analysis procedure

This document assumes that all images were taken in digital format. The procedure steps for a specific open source software are as follows.

NOTE The open source software is ImageJ, available from https://imagej.nih.gov/ij/download.html,

— Create working copies of all images/frames (preserve the original unmodified images).

— Open ImageJ and open the frame file.

— Set the measurement scale using the scale bar or another measurement of pixel size, returning to the original scale prior to continuing.

— Crop the image to remove scale bars and other image artefacts that might affect contrast or particle analysis.

— Check and correct brightness and contrast to ensure that all images have histograms centred and wide enough to cover at least 80 % of the possible grey levels.

— The thresholding operation may result in frame files with single pixel artefacts or poor image quality, e.g. rough particles or uneven background due to non-uniform electron beam illumination. In the case of the former, apply the despeckle and erode/dilate processes to remove these artefacts and save the changes. In the case of poor image quality, the operator could clean up the edges of particles or correct for uneven background by applying special filters. Assess the image transformation and save changes.

— Touching particles should not be addressed by using automated separation algorithms without determining whether the means and spreads of the resulting descriptor distributions are altered beyond acceptable measurement uncertainties. Touching particles may be separable from the raw dataset by applying appropriate shape or size factors to the raw data.

— Set the list of measurands desired (such as area, shape descriptors, Feret's diameter and fit ellipse). The available list of size and shape descriptors will vary by software. It is generally useful to select more descriptors than might be needed as the most repeatable descriptors may not be the one that

are conventionally reported for the specific particles. Multiple size and shape descriptors can be used to identify imaging and measurement problems as well as assist with the characterization of the particle sample under study.

— Analyse the particles (ImageJ specific settings should include: show outlines, display results, include holes, and exclude on edges).

— Save each image file that shows particle outlines and their number sequence (filename.tif) and the spreadsheet (Results.xls, with all descriptor values for all particles plus particle number and frame number).

NOTE Additional guidance can be provided based on findings from the case studies. Several case studies show intra- and interlaboratory data assessment procedures [e.g. analysis of variance (ANOVA)] that can be used to tune protocols for low measurement uncertainty values.

9 Data analysis

9.1 General

There are several major applications for statistical analysis of particle size data, including analysis of particle size data, assessment of data variation under repeatability, intermediate precision, reproducibility conditions of measurement, fitting reference models to the size distributions, and assessment of grand statistics for the entire study. Table 3 summarizes the methods used in this document. Measurement uncertainties are computed from coefficients of variation determined from the fitted parameters of each dataset in the ILC. Seven case studies of particle size and shape distributions by TEM are given in Annexes B to H. Key findings of these studies are summarized in Annex A.

Table 3 — Statistical analysis methods

Statistical method	Reported statistics
ANOVA	p-values: there is no difference between the mean value of the descriptor for a specific dataset and the grand mean value of the descriptor for all datasets.
Pair-wise ANOVA	p-values: there is no difference between the mean values of the descriptor for the data-set pair.
Bivariate analysis	p-values, energy values: pair-wise comparison of descriptor cumulative distributions; there is no difference between the descriptor distributions of the dataset pair; pair-wise comparison of size-shape distributions: there is no difference between the descriptor distributions of the dataset pair.
Fitting reference models to size distributions	Maximum likelihood and non-linear regression methods: fitted mean and spread parameter estimates plus their standard errors.
Kolmogorov-Smirnov	$D_{m,n}$ values: non-parametric differences between cumulative distributions; distribution pairs with differences greater in absolute value from the supremum are deemed to be different.

9.2 Raw data triage — Detecting touching particles, unselected particles, artefacts and contaminants

It can be useful to perform data screening, or “triage”, prior to full analysis of datasets. For example, touching particles and unselected particles should be removed from the dataset, artefacts should be identified and removed, and contaminants should be identified and analysed separately. Raw data triage workflows can be developed at the inception of a particle size and shape distribution project. An example of the raw data triage workflow is shown in Figure 5. The starting point is the raw data generated using ImageJ and the endpoint is a reduced dataset of only nanorod data conforming to the minimum area (> 200 pixels) constraint. The raw data contained the target nanoparticles (nanorods) plus nanocubes and some additional unselected particles. In this case study, touching particles were deemed to be undesirable. A heuristic was developed to identify touching particles using a defined

range of values for a specific descriptor. Particles within this range were extracted from the dataset and discarded. A second heuristic was developed to detect non-nanorods and other unselected particles. The nanocube dataset was retained for further analysis. Finally, the remaining nanorod data was sorted to remove particles with areas less than 200 pixels. The final product of this workflow can be taken through the rest of the data analysis pathway.

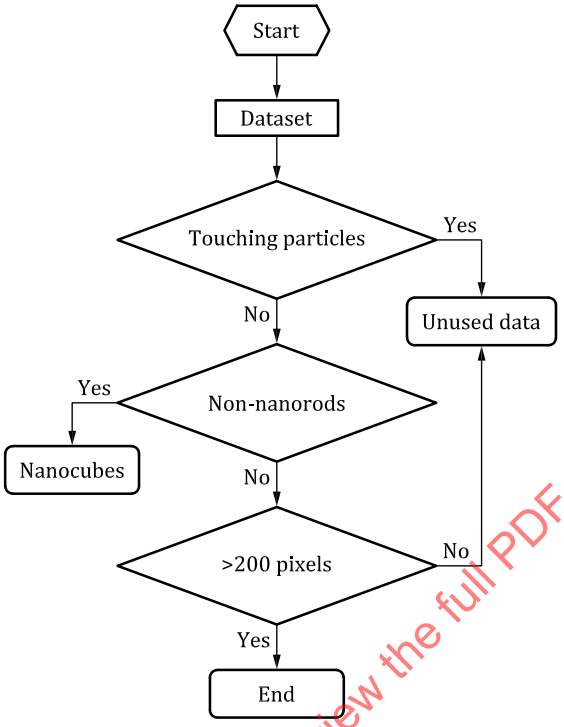

Figure 5 — Example of raw data triage for gold nanorod sample (see Annex D)

Commonly used distributions require at least two parameters: one that describes mean (or size) and one that describes the spread (or shape) of the data. For each application, the relative standard error (RSE) needed for the mean and standard deviation of the distribution will set the number of nanoparticle images required. The methods for curve-fitting distributions to particle size data in this document (see 9.2) provide RSEs for each of the two descriptors (mean and spread). Assuming that the fitted distribution provides a good description of the data, investigators can determine the effect of the number of particles analysed on the RSEs for their samples and adjust the number of particles counted to develop datasets with the needed accuracy.

For size and shape descriptors, ISO 9276-6:2008 provides sets of size, proportion and mesoshape descriptors that are commonly used to define particle morphology and that shall be used. Particles can be characterized with size and/or shape descriptors. Particle populations often have unique size/shape descriptor ranges, providing a pathway to identifying and separating aggregates, agglomerates, artefacts, and/or foreign particles from captured particle datasets.

9.3 Data quality assessment — Repeatability, intermediate precision and reproducibility

A key objective of ANOVA is to identify particles, frames or datasets to review, usually by visual inspection of the image and its thresholded data. ANOVA can be used to assess the intralaboratory repeatability, intermediate precision and interlaboratory reproducibility. At typical specified resolutions, there are usually a small number of nanoparticles in any given view frame; 20 to 100 particles might be common. For this number of points, average descriptor values can be computed for each frame. However, it is not likely that reasonable estimates for size distribution parameters, i.e. the mean and spread of the distribution, can be computed for one frame. Table 4 summarizes the null hypotheses and metrics

for each of these assessment types. The p-value statistic is used as the metric for each, and, for this document, freeware was used for the ANOVA method (see https://shiny.as.uky.edu/anova-app/).

Table 4 — Data quality assessment by ANOVA

Data quality assessment	Null hypothesis	Metric
Intralaboratory repeatability – same operator, same day	Do all images have the same descriptor mean as its grand mean?	if $p < 0,05$, the null hypothesis is rejected
Intermediate precision – different operator or different day	Do all datasets have the same descriptor mean as its grand mean?	if $p < 0,05$, the null hypothesis is rejected
Interlaboratory reproducibility – different laboratory, different operator	Do all datasets have the same descriptor mean as the grand mean?	if $p < 0,05$, the null hypothesis is rejected

Figure 6 shows a workflow for interlaboratory repeatability assessment during a raw data triage. In this case, the null hypothesis is that a specific descriptor mean for each image is the same as its grand mean for all images. When all images are analysed (A_1 through A_n), an ensemble or grand mean of the descriptor is determined for the entire dataset and the descriptor means for each frame are compared to the grand mean. A typical output of the software is a boxplot showing the grand mean, an average descriptor value for each frame, a boxplot for each frame (typically a box indicating 75 % of the descriptor values; ±1,5 *s*) and extreme points. If needed, the extreme points can be viewed on the frame images to ensure that they are the desired nanoparticles and not artefacts or contaminants.

In general, a particle and its associated data should be reported and should not be discarded from the dataset unless:

— the particle image is found to be corrupted;

— the particle image is determined to be an artefact; or

— the particle is determined to be a different class/type than the assay is trying to count.

In general, an image and its data should be reported and should not be discarded from the dataset unless:

— the calibration or other instrument operating settings are found to be different from the standard.

A statistic that indicates a particle is “extreme” is not a sufficient reason to cause the particle to be discarded. This analysis can be repeated for all recorded descriptors. The repeatability of various descriptors can be compared by ranking their p-values, or by determining the fraction of frames which have descriptor means similar to the grand average. Either method helps to demonstrate which descriptors are well-known for the dataset.

The decision tree of Figure 6 can be applied to intermediate precision and reproducibility evaluations. For the latter, the A_i datasets are those of the ILC members. In addition, pairwise comparison of datasets also provides information on the similarity of dataset means. A statistical test alone is not sufficient reason to discard data.

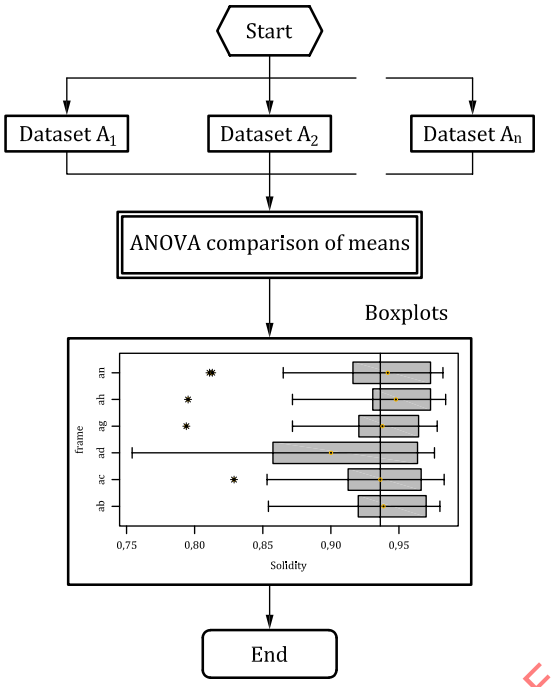

NOTE This boxplot shows the repeatability analysis of the solidity descriptors for six frames of carbon black aggregate images.

Figure 6 — ANOVA workflow for repeatability and reproducibility analysis

9.4 Fitting distributions to data

Preferred reference models for the descriptors of samples may not be known. Non-linear regression methods can provide estimates for the reference distribution parameters and their standard errors. The preferred reference model for a specific dataset would generally have parameter estimates with the lowest relative standard errors. The methods of this document can be used to select the best reference distribution or to identify descriptors that have low relative standard errors.

Size descriptors report the dimensions of the particles while shape descriptors report the shapes of the particles. Each descriptor is fitted to a reference model with two parameters: a mean parameter that reports a characteristic value for the size/shape descriptor and a spread parameter that reports the spread of the fitted distribution model.

Three reference models are commonly fitted to cumulative particle size distribution data: normal, lognormal and Weibull. Note that, for each of these reference models, the computation of the mean and spread parameters are distinct and different. For convenience, the characteristic value of the descriptor is called the "mean", and the characteristic breadth of the distribution is called the "spread". Fitting reference models to cumulative distributions is usually preferred. Differential probability distributions lose information when the data are binned, often obscuring the details near the tails of the distributions. In general, parameter values from cumulative distribution fits have lower relative standard errors than those for binned differential distributions.

Three non-linear regression methods (in accordance with ISO 9276-3) shall be used to fit data to the cumulative distribution and to optimize the values of fitted parameters:

— minimizing the variance between the data and reference model;

— setting the residual deviations between the data and reference model to zero;

— transforming the three reference models into linear functions (quasilinear regression).

Commercial statistical software can provide the R^2 value for the preferred fit, the parameter estimate [e.g. mean ($\bar{x}$) and standard deviation (s)], and the standard error of the parameter estimate ($u_{\bar{X}}$ and u_S). The relative standard error (RSE, the standard error divided by its statistic) is a measure of the quality of the parameter, with smaller values being better.

Free software (see https://shiny.as.uky.edu/curve-fitting-app/) was used to fit distributions to data. This method provided a consistent analysis approach for all datasets. Figure 7 shows the model fitting workflow used for the case studies of this document (see Annexes B to H).

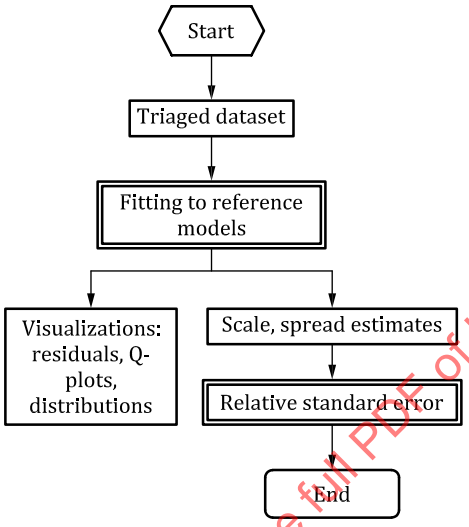

Figure 7 — Workflow for fitting particle size and shape distribution models to measured data

The dataset used for estimating mean and spread parameters can be from a single laboratory or test day, or assembled by combining all datasets in the study, across different test days and/or laboratories. Using the freeware tool, the user can select one of three different reference models, and estimate the best fitted parameters by one of two methods: non-linear regression or maximum likelihood. The relative standard error of the mean and spread parameters can be calculated for each estimation method and each model. When one reference model has a significantly lower relative standard error for both descriptors, it may be the preferred choice.

9.5 Assessing measurement uncertainty for samples under repeatability, intermediate precision or reproducibility conditions

9.5.1 Grand statistics for fitted parameters — Three or more datasets

Estimates of the fitted parameters for each descriptor can be generated for each dataset by the method given in 9.3. Assuming that the fitted parameter values are normally distributed, the "grand statistics" for all datasets are computed: the mean, standard deviation and coefficient of variation for each fitted parameter of a descriptor. The grand coefficient of variation for each fitted parameter should relate to its relative measurement uncertainty. This approach does not differentiate between material homogeneity (sample-to-sample) and method precision (repeatability, intermediate precision or reproducibility).

9.5.2 Measurement uncertainty of fitted parameters

There are different approaches to the evaluation of the uncertainty of measurement[36][37][38] and of the precision and bias of methods. The ISO/IEC Guide 98-3 approach to measurement uncertainty is to define the measurands, identify all relevant sources of uncertainties in the test, quantify each significant source of uncertainty with a probability distribution, calculate the combined (pooled) standard uncertainty, and estimate the expanded uncertainty at a specified confidence level. Some references provide great detail on measurement uncertainty for measurement of particle size alone[25][27][28][29][30]. Here, the GUM-compliant approach of Braun et al.[39] is followed.

Type A uncertainty components include those that are evaluated by statistical methods, such as of repeated tests or tests on CRMs. Type B uncertainty components are evaluated by other means, such as calibration errors or effects of temperature variations. The Type A components are:

— the degree of closeness of measurement to the reference value;

— the precision (the degree to which different measurements show the same result).

Precision is usually separated into two components: repeatability (the variability observed for the same operator and same instrument) and reproducibility (the variability observed for the same process being performed by different operators on different instruments), as in the case studies in the annexes. When an RM is being investigated for its certified descriptor, the trueness can be computed [the difference between the certified value and the average descriptor value (bias)].

9.5.3 Example — Measurement uncertainty for a size descriptor

For a size descriptor, the pooled measurement uncertainty, $u_c(x)$, is based on the interlaboratory reproducibility $u(ir)$, the trueness, $u(t)$, and the instrument calibration error, $u(c)$. $U(ir)$ and $u(t)$ are Type A uncertainty components while $u(c)$ is a Type B uncertainty component. The pooled measurement uncertainty is the square of the sum of the squares of its individual components, as shown by Formula (1):

$$u_c(x)=\sqrt{u(ir)^2+u(t)^2+u(c)^2} \tag{1}$$

9.6 Bivariate analysis

Bivariate analysis can be used to compare two-dimensional datasets independent from an assumed model but does not lead to calculations of measurement uncertainty. However, it does provide statistical measures of distribution similarity; it may be useful in some cases. Several of the case studies in the annexes include particles with both size and shape variations. Considering both types of descriptors is important to the characterization of such materials. Figure 8 shows the workflow for bivariate analysis[40]. This method is a nonparametric test for equal distributions in high dimension, testing the composite hypothesis of equal distributions when the distributions are unspecified. Several types of two variable comparisons can be analysed by this method: empirical distributions (descriptor–cumulative distribution data) and descriptor–descriptor data (size–size, size–shape, or shape–shape). The bivariate method is very useful for statistical comparison of datasets but does not provide metrics that can be used to compute measurement uncertainty of descriptors.

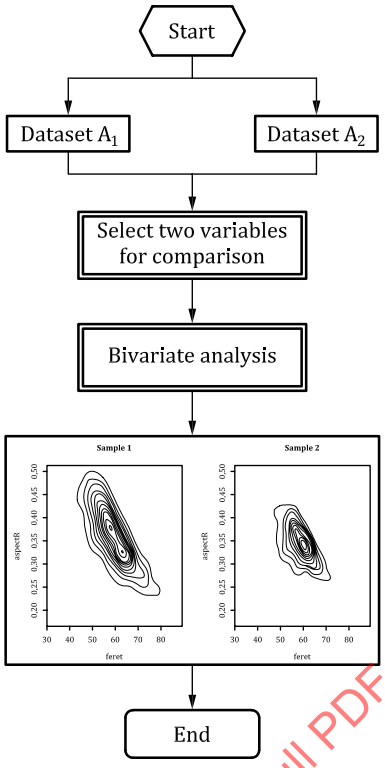

NOTE This bivariate analysis compares the aspect ratio versus Feret diameter for two different gold nanorod samples ($p < 0{,}001$ for this pair of samples).

Figure 8 — Workflow for bivariate analysis of dataset pairs

10 Reporting

Table 5 is an example reporting template based on the workflow and decision tree guides of this document. Template sections include: frontpiece, sample preparation, instrument factors, image capture and particle analysis, and data analysis. Inserts in light grey are example responses or comment prompts. The actual reporting template shall be tailored to the sample and its application.

Table 5 — Example reporting template (example entries are shaded in grey)

Frontpiece

Project element	Response
Study title	
Study objective	
Laboratory	
Author	
Date submitted	

Sample preparation

Item	Comments
Sample ID	
Date received	
Substrate	
Sample type	Powder, dispersion

Table 5 *(continued)*

Sample condition	Optically clear dispersion, turbid dispersion, …
Sample treatment	
Sample division/splitting	
Grid pretreatment	
Particle deposition	
Incubation	
Washing	
Staining	
Drying	
Substrate	Type of substrate, substrate pretreatment, …
Placement method	
Drying method	

Instrument factors

Item	Comments
Organization	
Operator	
Analysis dates	
TEM instrument manufacturer	
Instrument model	
Operating voltage	
Beam current settings	
Objective lens excitation	
Diffraction aperture	
Calibration standards	
Calibration procedure	
Most recent calibration date	

Image capture and particle analysis

Item	Comments
Image capture	
Software/method	Software/manual or automated acquisition
Measurement conditions	Magnification, nm/pixel, frame size, signal-to-noise ratio
Descriptors retained	Itemize all measurands analysed, number of particles reported, number of frames
Particle analysis	
Thresholding conditions	
Minimum particle area (> 200 pixels)	
Number of frames, particles	

Table 5 *(continued)*

Data analysis

Item	Comments
Raw data triage	
Software/method	
Detection of touching particles	Report descriptors, ranges for detection and differentiation
Detection of artefacts	Report descriptors, ranges for detection and differentiation
Retained particles	Report descriptors, ranges for detection and differentiation
Average yield, %	Report the % of particles retained
Other triage steps	
Repeatability, intermediate precision or reproducibility	
Software/method	Software/ANOVA; bivariate analysis; other
Repeatability, intermediate precision or reproducibility	Report p-value for grand mean analysis; % similar p-values for pairwise analysis
Descriptor selection	Report method for description selection, if applicable
Fitting distributions to data	
Software/method	Software/non-linear regression; maximum likelihood; other
Preferred reference model	Report normal, lognormal, Weibull, or other distribution
Parameter values	Report estimates and standard errors, C_v %
Measurement uncertainty	
Descriptor residual standard error	Report descriptor parameter residual standard error if computed
U_{ILC} or U_{ip}	Report interlaboratory measurement uncertainty if computed
Residual deviations; correlations	
Software/method	
Residual standard deviation	Report if computed
Plots: residual deviations, quantile, other	Report residual deviation plot, quantile plot, … showing range over which the model fits the data
Correlations	Report correlations developed between descriptors

Annex A
(informative)

Case studies overview

A.1 General

Detailed procedures were validated with round robin studies (see Annexes B, D, E and F) conforming to VAMAS guidelines for ILCs [41][42] and ISO 5725-1.

Key findings reported in each case study annex are given in Table A.1.

Table A.1 — Key findings reported in each case study annex

Annex	Key findings
Annex B, Discrete spheroidal nanoparticles	Data quality is assessed for automated image capture; measurement uncertainties are reported for distribution means and spreads
Annex C, Size mixture	Criteria are demonstrated for separating bimodal data into clusters and evaluating the intermediate precision of separated clusters
Annex D, Shape mixture	Criteria are demonstrated for identifying touching nanorods and quantifying differences in size and shape distributions
Annex E, Amorphous aggregates	The measurement uncertainties of aggregate descriptor distribution means are in the order: elongational shape < size < ruggedness. Spheroidal, ellipsoidal, branched and linear aggregates are non-uniformly distributed, leading to multimodal distributions
Annex F, Nanocrystallite aggregates	Manual outlining of nanocrystallites is reported. Calibration method and imaging software did not affect some size and shape descriptor quality. Size descriptors are often better represented by lognormal distributions. Bimodal modelling of a size distribution is an example of visualization techniques used for improved understanding.
Annex G, Nanofibres with irregular cross-sections	Three manual measurement methods are compared with data for elemental fibrils of cellulose nanocrystals, which are low aspect ratio particles.
Annex H, Nanoparticles with specific crystal habits	Reproducibilities for two-dimensional images of three-dimensional particles are compared by ANOVA for three instrument types, multiple analyses of one grid, and analysis of the same particle images by six laboratories.

A.2 Discrete spheroidal nanoparticles (see Annex B)

RM8012 is an RM of spheroidal gold nanoparticles that is often used for TEM calibrations[35][38].

A.3 Size mixture (see Annex C)

Colloidal silica is used for polishing slurries, as an additive to cosmetics and as a component in nanocomposites. The sample was a CRM (ERM-FD102), a bimodal mixture of commercial colloidal silicas[36][37].

A.4 Shape mixture (see Annex D)

The tunable, longitudinal plasmon resonance of gold nanorods has been linked to their morphology[43]. Two mixtures of gold nanorods plus gold nanocubes were thought to have different performance properties[44]. The samples were similar to a National Certified Standard Material in China.

A.5 Amorphous aggregates (see Annex E)

Carbon black aggregates have aciniform morphology, in which nodules (constituent features that have been called "primary particles") are aggregated into "grape-like" clusters. Cabot Corporation supplied a carbon black reference sample, SRB8, for which an existing protocol (ASTM D3849-14a[24][45]) was available.

A.6 Nanocrystallite aggregates (see Annex F)

Nanocrystalline metal oxides are in common use and are almost always aggregated when manufactured in a vapour phase process. The size and shape of the constituent crystallites of aggregated titania powders are essential to product performance. Tayco Corporation supplied a commercial sample.

A.7 Low aspect ratio particles (see Annex G)

Size and shape distributions of low aspect ratio nanoparticles are critical to a number of their applications. Measurement methods are reported for the elementary fibrils of a cellulose nanocrystals CRM supplied by National Research Council, Canada (CNCD-1[46]).

A.8 Nanoparticles with specific crystal habits (see Annex H)

Bipyramidal titania nanoparticles have well-defined three-dimensional crystallite morphologies[47] and are being considered as a potential RM for both size and shape distributions.

Annex B
(informative)

Discrete spheroidal nanoparticles

B.1 Reference

A complete report of the method and results is given by Rice et al.[26].

B.2 Background and design objectives

RM8012 (30 nm nominal size) is an RM prepared by NIST. Figure B.1 shows a typical TEM frame with gold nanoparticles. A number of particles are touching. As the gold nanoparticles are faceted, not all profiles are round. The protocol included automated image capture, automated particle analysis, and statistical analysis of the raw data and distribution fitted parameters, providing a framework for measuring particle size distributions.

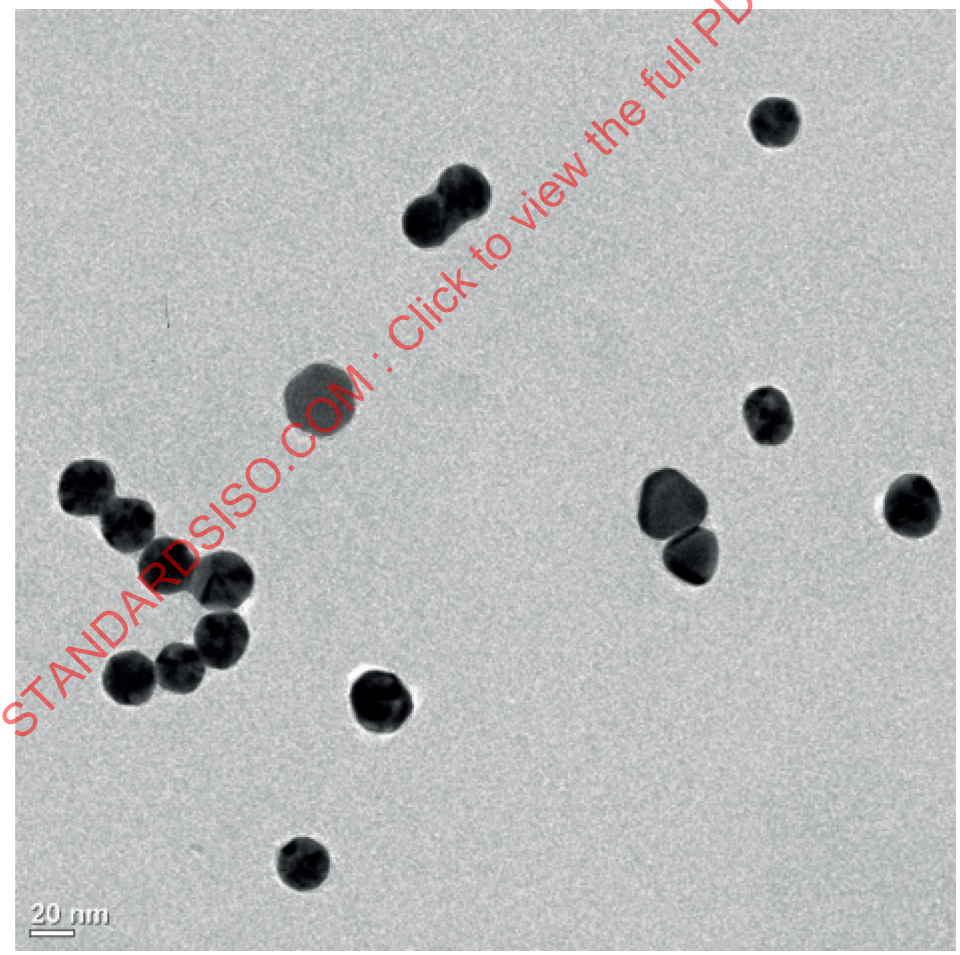

Figure B.1 — A TEM image of RM8012

B.3 Highlights

Intralaboratory repeatability of ECDs, Feret diameters and aspect ratios was satisfactory as assessed using ANOVA of frame data.

Table B.1 shows the measurement uncertainties (U_{ILC}) of fitted model parameter for both the lognormal and normal distributions for an ILC[26]. The mean parameters of lognormal models fitted to the distributions have the lower measurement uncertainties than those for normal model: U_{ILC} = 1,6 % and 5,5 %, respectively. The spread parameters (width of the distribution) for each distribution model have similar coefficients of variation and measurement uncertainties. The measurement uncertainty of the arithmetic means (averages) is even higher than that for the fitted normal distribution values.

Table B.1 — Measurement uncertainties of fitted model parameters for ECD descriptor

Statistic	Mean parameter	Spread parameter
Lognormal distribution	X, ln(nm)	S, ln(nm)
C_v, in %	0,76 %	6,0 %
U_{ILC}, in %	1,6 %	12,6 %
Normal distribution	X, in nm	S, in nm
C_v, in %	2,6 %	5,8 %
U_{ILC}, in %	5,51 %	12,3 %

An ImageJ subroutine for separation of touching particles gave size distributions with smaller mean parameters and narrower spread parameters. Figure B.2 shows the maximum Feret diameter distribution for non-touching particles alone (black squares) and non-touching and touching particles separated by Watershed algorithm (red open circles). The mean value for the non-touching data is several per cent higher than that of the separated data. In addition, the spread of the non-touching particle distribution is wider than that of the touching data. In this case, the use of the Watershed algorithm to separate touching particles leads to quantitatively different distributions.

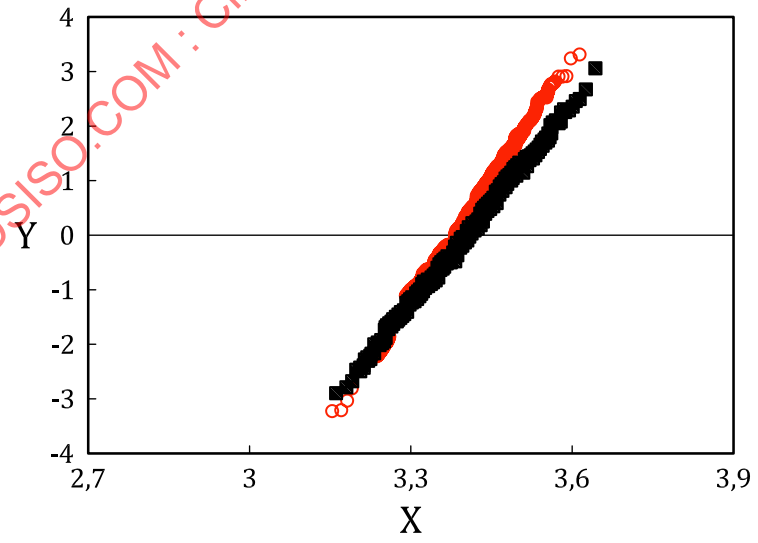

Key

■ non-touching particles

○ touching particles

X = ln(ECD particle size x)

$$Y = \frac{1}{s} X - \ln \frac{x_{50,r}}{s}$$

Figure B.2 — Quantile plot of maximum Feret diameter distributions of non-touching particles and touching particles distributions (separated with a software algorithm)

Size descriptors had similar measurement uncertainties. Either the ECD and Feret diameter would provide similar representations of the test sample's size distribution. Lognormal models provided lower measurement uncertainty values for the mean and spread parameters of size distributions than normal reference models. While the sample is certified for its average equivalent diameter (which assumes a normal distribution), the measurement uncertainty is lower for the mean value of a lognormal distribution.

Annex C
(informative)

Size mixture

C.1 Purpose

Nanoparticle materials can have a multimodal size and/or shape distribution, either as an immediate result of the nanoparticle processing method, or as the result of mixing different nanoparticle materials. This annex provides examples of how to treat electron microscopy size and shape data obtained on such materials. It may, for example, be important to separate different fractions (or "modes" or "clusters") in a particulate material before performing an analysis of the individual fractions.

C.2 Background and design objectives

The material chosen to illustrate the possible approaches is ERM-FD102[36], a CRM produced by the Joint Research Centre (JRC) of the European Commission. ERM-FD102 was prepared by mixing two commercial colloidal silicas with different nominal sizes, ≈20 nm and ≈80 nm. For both main modes in the CRM's particle size distribution, the CRM certificate[36] provides several method-defined certified particle sizes for both main modes of the CRM's particle size distribution, including electron microscopy analysis (see Figure C.1). Since the sizes of the main modes differ by a ratio of about ≈4, different magnifications were used in the electron microscopy characterization of the CRM to obtain representative size distributions for both modes. Each electron microscopy laboratory participating in the CRM characterization study obtained six datasets over a three-day period, with least 300 large particles in each dataset.

The median ECD by electron microscopy, certified for the larger of the two modes in ERM-FD102, is 83,3 nm with an expanded measurement uncertainty of 2,3 nm. This value is the median value over the size range of 60 nm to 120 nm[36]. The width of the corresponding peak in the particle size distribution was not certified.

AFM images of the same material (ERM-FD102)[37] also show the presence of mid-sized particles between the large particles (nominally 80 nm) and the small particles (nominally 20 nm). TEM images taken to measure the large particle cluster also show the "mid-sized" silica particles in the range of ≈40 nm. Figure C.2 shows a histogram and a cumulative distribution from the TEM data of one reporting laboratory ("Lab 1"): the total number of large particles reported in the range from 35 nm to 125 nm was 2 801, with 761 of them having ECD sizes less than 60 nm; this value corresponds to the apparent minimum between the two peaks of the histogram. All size descriptor distributions for ERM-FD102 are bimodal. Three types of descriptors were reported: size (including area, perimeter, Feret diameter, minimum Feret diameter and ECD), elongational shape (including aspect ratio and compactness), and ruggedness/boundary irregularity (including form factor and solidity).

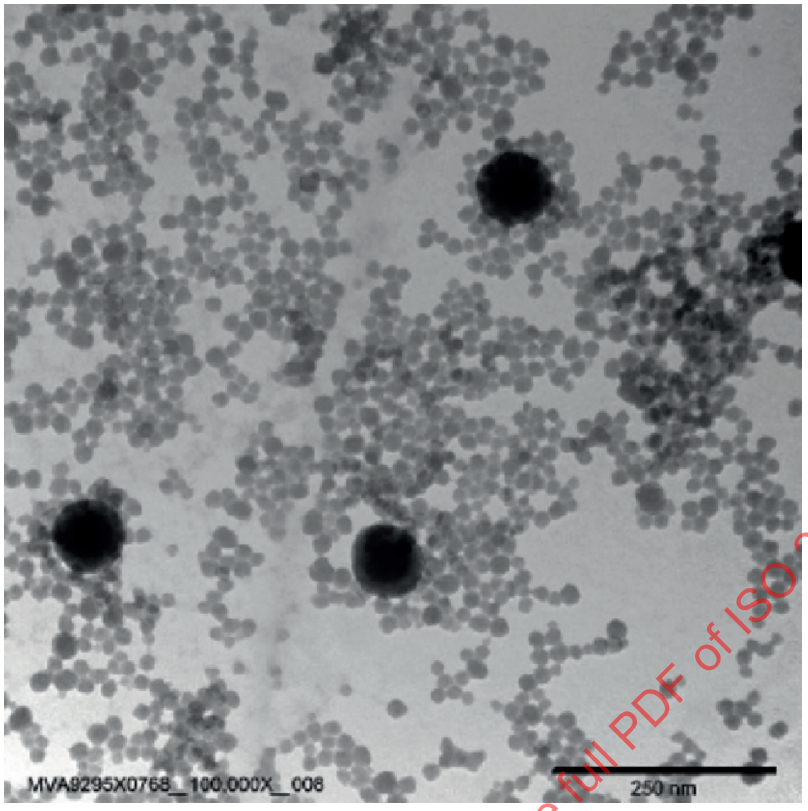

NOTE Used with permission of the Joint Research Centre of the European Commission (JRC).

Figure C.1 — TEM image of a mixture of colloidal silica nanoparticles

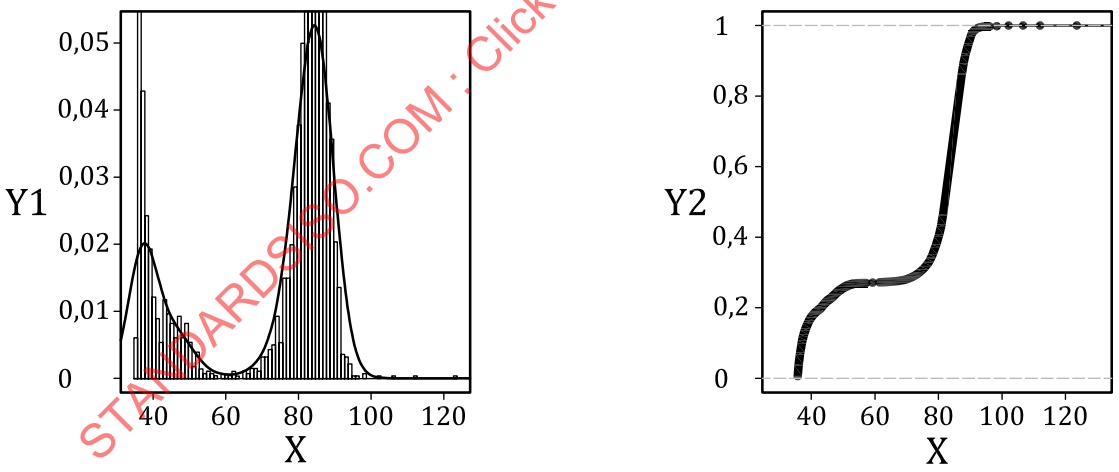

a) Density distribution **b) Cumulative distribution**

Key

X ECD, in nm

Y1 density distribution

Y2 cumulative distribution

NOTE Histogram (left hand side; density distribution as continuous black curve) and cumulative distributions (right hand side; points as solid circles, cumulative distribution as continuous black curve).

Figure C.2 — Density and cumulative distributions from analysis of large particle images, ECD (Lab 1)

Table C.1 shows the sample IDs, the number of particles counted between 35 nm and 125 nm, the number of the particles with an ECD larger than 60 nm, and the fraction of particles with ECD < 60 nm. All datasets reported more than 300 large particles analysed (an objective of the protocol) except for D3S1, which reported 271 of the large particles. The average fraction of the mid-sized particles was 27,2 %.

Table C.1 — Six datasets for intermediate precision comparisons

Dataset			**particle counts**		
Day	Sample	ID	All	ECD > 60 nm	ECD < 60 nm, %
1	1	D1S1	472	341	27,8 %
1	2	D1S2	411	330	19,7 %
2	1	D2S1	509	367	27,9 %
2	2	D2S1	510	369	27,6 %
3	1	D3S1	418	271	35,2 %
3	2	D3S2	481	362	24,7 %
		totals	2 801	761	

C.3 Highlights

C.3.1 General

This analysis addresses three questions:

a) what methods can determine similarities or differences between bimodal size distributions?

b) what methods might best differentiate between the large particles (nominally ≈80 nm) and the mid-sized particles (nominally ≈40 nm)?

c) what are the intermediate precisions (see Table 4) of the size, elongation and ruggedness distributions?

Answers to the first question will establish steps for raw data triage. Answers to the second question can be automated to separate the data into large and mid-sized particle clusters. The intermediate precision answers for large particles can be compared to the measurement uncertainty values of the CRM[36][37].

C.3.2 Raw data triage

In the ERM-FD102 characterization study, laboratories reported six datasets taken over a three-day period (two per day). The comparison of sample means by an overall ANOVA is not particularly relevant if one wants to judge the equivalence or comparability of two measured bimodal distributions. Instead, pairwise ANOVAs were done for each of the 15 possible pairs for six datasets D_iS_j (e.g. as in Table C.1). ANOVA pairwise comparisons of ECD (size), aspect ratio (elongational shape), and solidity (ruggedness shape) gave $p > 0,05$ for 11 of 15, 15 of 15, and 9 of 15 pairs, evaluated as very good (ECD), excellent (aspect ratio), and good (solidity) intermediate precision. Since the dataset means are intermediate between the nominal diameters of the mid-sized and large particles, these mean values are sensitive to the number fractions of each category reported in Table C.1.

Methods that compare distributions directly would be more appropriate for comparing these datasets, such as bivariate analysis and Kolmogorov-Smirnov (K-S) analysis. The K-S test is designed to determine directly whether two cumulative distributions are dissimilar, without reference to any particular model that might describe the data. The cumulative distribution for each dataset was binned using 100 equal steps over the total data range for each descriptor. Differences between two curves at each step, $D_{m,n}$, were compared to the supremum statistic (see Table 3[44][48]). If the difference exceeds the supremum, the cumulative distributions are judged to be different. Figure C.3 a) shows the cumulative distributions for three datasets: A, B and C.

The supremum values for these three pairs were similar, ≈0,09, so only one set of supremum values (both + and −) were plotted in Figure C.3 b). By the K-S test, all three of these datasets have areas that exceed the supremum and are judged to be different. This is due, in part, to the differences between the number of mid-sized particles in the various datasets, which varied from ≈20 % to ≈35 %. It is likely that such differences could be reduced if the number of data points were increased. The K-S test would be preferred to the ANOVA test for these bimodal distributions as it provides better information about differences between distributions ($D_{m,n}$) and, specifically, how these differences vary along the descriptor range.

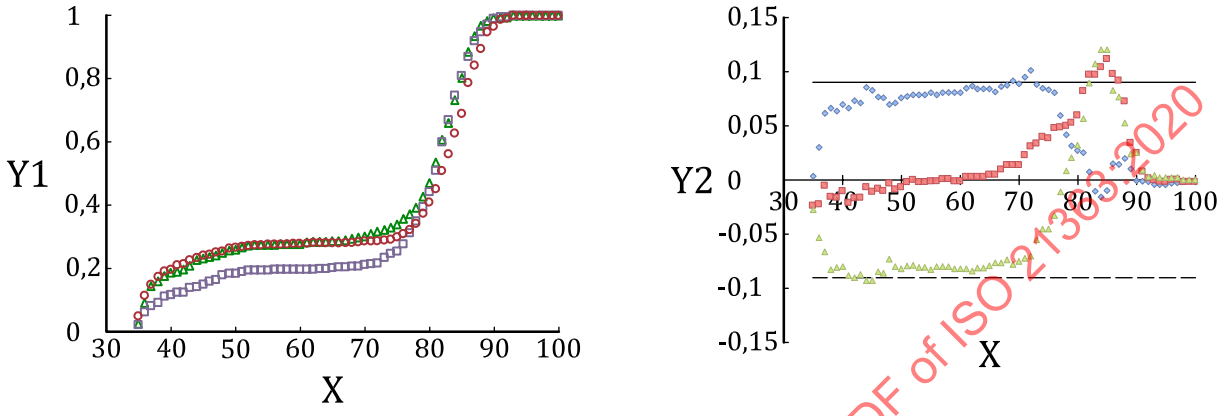

a) Cumulative ECD distributions **b) K-S cumulative curve pairwise differences**

Key

- sample A
- sample B
- sample C

X ECD, in nm
Y1 cumulative distribution
Y2 $D_{m,n}$

NOTE 1 Cumulative ECD distributions of three different samples, A (green open triangles), B (purple open squares) and C (red open circles), suggests that samples A and C are similar.

NOTE 2 Kolmogorov-Smirnov analysis shows that all three pairs have differences greater than the supremums and are statistically different.

Figure C.3 — Repeatability analysis of three ECD bimodal datasets

Similar plots for the elongational shape distributions (aspect ratio) are shown in Figures C.4 a) and b). The aspect ratio distributions for all imaged particles are multimodal. The aspect ratio distribution has considerable variability for values up to 0,9, see Figure C.4 a). This is caused by two factors: differences in the aspect ratio distribution for the two clusters, and differences in the fractions of each cluster in the overall distribution from sample to sample. The two datasets with similar fractions of the mid-sized cluster, A and C (with 27,8 % and 27,9 %, respectively), have $D_{m,n}$ values well within the supremums over all values of the aspect ratio ranges. Two of these three dataset pairs are judged to have similar aspect ratio distributions.

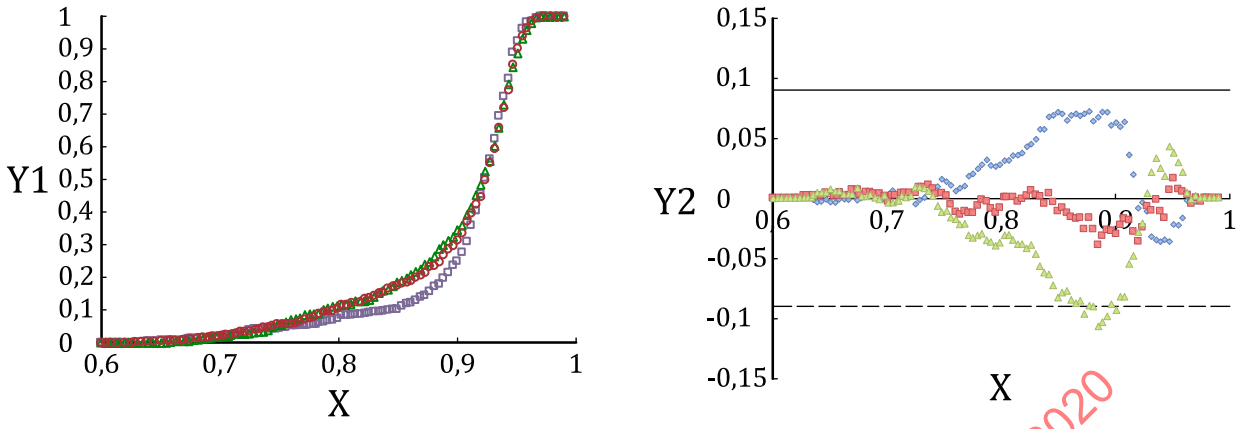

a) Cumulative aspect ratio distributions **b) K-S cumulative curve pairwise differences**

Key

- sample A
- sample B
- sample C

NOTE 1 Cumulative ECD distributions of three different samples (A (green open triangles), B (purple open squares) and C (red open circles) suggests that samples A and C are similar.

NOTE 2 Kolmogorov-Smirnov analysis shows that all the pair, A-C (green triangles) have differences greater than the supremums and are statistically different.

Figure C.4 — Repeatability analysis of three aspect ratio datasets

C.3.3 Differentiating between large and mid-sized particle clusters

C.3.3.1 General

The two data clusters shown in Figure C.2 can be separated in several ways, including a minimum value in the ECD distribution, which is the range of 60 nm. Alternate approaches would consider both the size and shape of the colloidal silica particles. Colloidal silica particles are known for their spheroidal shapes. Nonetheless, three methods for considering particle size and shape correlations are shown here. The first considers a size–size correlation with the maximum Feret diameter as the independent variable and the minimum Feret diameter as the dependent variable. The others use the ECD diameter as the independent variable with either an elongational (aspect ratio) or ruggedness (solidity) shape descriptor as the dependent variable.

Size–size correlation: Figure C.5 shows a plot of the minimum Feret diameter as a function of the Feret diameter. The two clusters have been separated empirically using the dashed line to automate the sorting process. In this case, a number of lines could be used to do the separation, from vertical to horizontal. Linear models (minFeret = a × Feret + b) for each of the clusters give different slopes, but the correlations have R^2 values of 0,76 and 0,66; their equations are not reported here as they do not provide a convincing method for differentiating the two particle clusters.

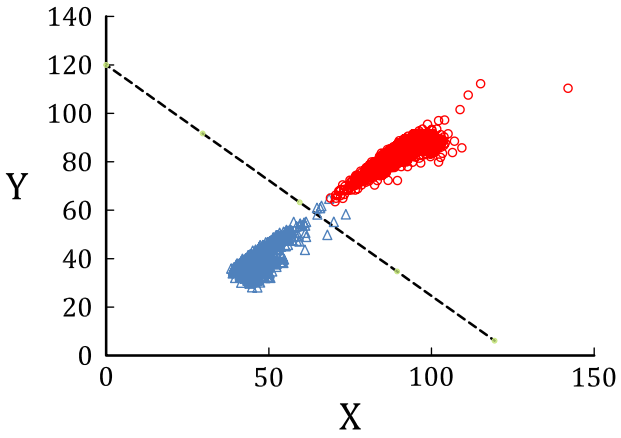

Key

○	(2 034 particles) – large particles	X	Feret, in nm
△	(767 particles) – mid-sized particles	Y	minFeret, in nm
_ _ _	cluster boundary		

Figure C.5 — Size–size cluster analysis

C.3.3.2 Elongation–size correlation

An alternative method is to correlate the aspect ratio to the ECD diameter. The result is shown in Figure C.6 a). This plot shows morphology differences between the two clusters. The large particle cluster has a smaller aspect ratio range, ≈0,77 to 0,98. The mid-sized particle cluster has an aspect ratio range of ≈0,61 to 0,96. Therefore, more particles of the mid-sized cluster are elongated than those of the large cluster. However, the clusters cannot be separated using just their aspect ratio distributions, as there is significant overlapping of the ranges. The overlapping ranges contribute to the broad range of aspect ratio distributions seen in Figure C.4 a). In addition, the mid-sized cluster appears to be truncated for ECD < 35 nm; this issue is discussed more fully in C.3.4.

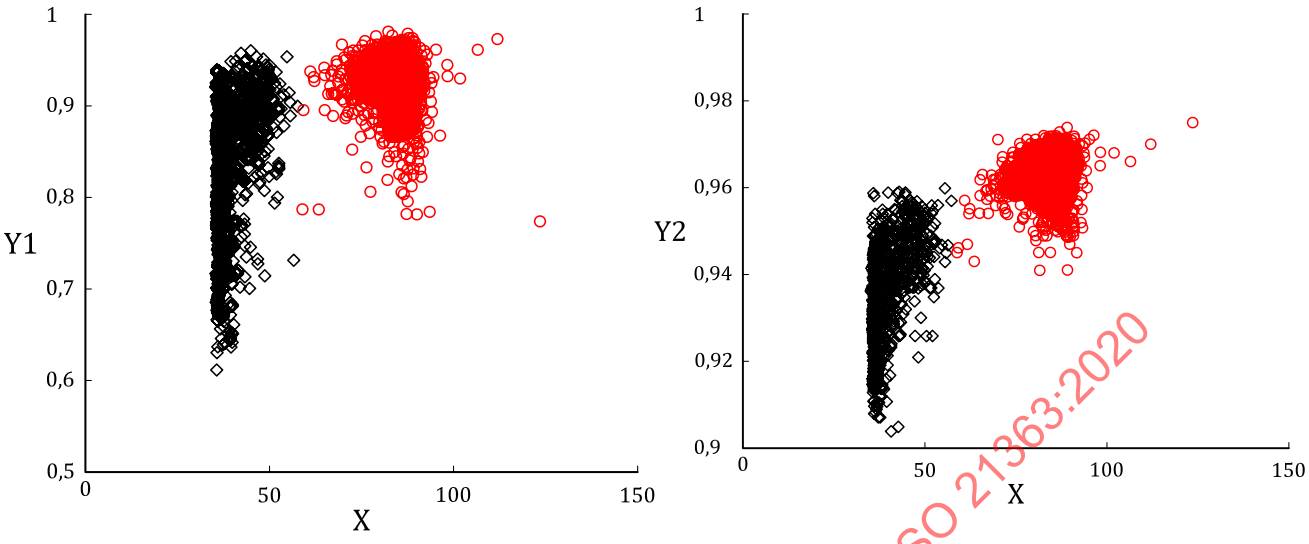

a) Aspect ratio versus ECD

b) Solidity versus ECD

Key

○ (2 034 particles) – particles

◇ (767 particles) – mid-sized particles

X ECD, in nm

Y1 aspect ratio

Y2 solidity

Figure C.6 — Correlations between ECD and two shape descriptors (elongational and ruggedness)

C.3.3.3 Ruggedness–size correlation

Figure C.6 b) shows the correlation between solidity and ECD for these two clusters. Solidity is a measure of surface ruggedness, or boundary irregularity. Solidity values for both clusters are fairly high, however, there is still a difference in the ruggedness descriptors. The clusters cannot be distinguished using solidity alone however, paired with ECD, there is a convincing distinction between the two. Choices for the boundaries between clusters in any of these correlations can be quantified for automated separations.

C.3.4 Laboratory intermediate precision

Intermediate precision values can be computed for the parameters of reference models fitted to the cumulative distributions of the large and mid-sized clusters separated by the method of Figure C.5. Tables C.2 and C.3 show the fitted parameters for ECD, aspect ratio and solidity for the large and mid-sized clusters, respectively. The average value for the large cluster ECD value is 84,1 nm and the spread of the data is 4,0 nm. The mean value has good correspondence to the median value reported for the large size particles (83,3 nm). There is no certified value for the spread of this distribution, or for the aspect ratio and solidity fitted parameters. The uncertainty of the ECD mean is 2,3 % and the uncertainties of the aspect ratio and solidity means are lower than this. The uncertainties associated with the spread of the data are much larger.

Table C.2 — Separated large particles — Fitted parameters for the mean and spread for ECD, aspect ratio and solidity distributions (2 040 images) — Normal reference model

Sample	ECD nm		Aspect ratio		Solidity	
	mean	spread	mean	spread	mean	spread
D1S1	83,9	4,01	0,935	0,021 7	0,963	0,003 5
D1S2	82,9	4,25	0,932	0,020 7	0,963	0,003 4
D2S1	84,9	4,05	0,935	0,022 6	0,963	0,003 6
D2S2	85,3	3,61	0,930	0,024 4	0,963	0,003 9
D3S1	83,6	4,08	0,932	0,021 7	0,964	0,003 6
D3S2	83,6	4,12	0,932	0,021 1	0,963	0,003 3
average	84,1	4,02	0,932	0,022 0	0,963	0,003 6
stdev	0,909	0,217	0,002 0	0,001 3	0,000 1	0,000 2
C_v, in %	1,08	5,39	0,22	6,02	0,01	5,84
U, in %	2,34	11,	0,47	13,0	0,02	12,6
U, value	1,96	0,47	0,004 4	0,002 9	0,000 2	0,000 4

Figures C.7 a) to c) show smoothed density distributions of the combined datasets of the fraction of large particles in ERM-FD102, along with models with parameters fitted using either non-linear regression or maximum likelihood estimations. All fits are based on normal reference models. The ECD data are fairly well-represented by a normal distribution, with slight differences in the peak value plus the leading edge of the distribution. The aspect ratio data are multimodal; there are significant deviations between data and model at the leading edge, the maximum and the trailing edge of the descriptor range. The solidity data are also multimodal but there is slightly better correspondence between the data and the models.

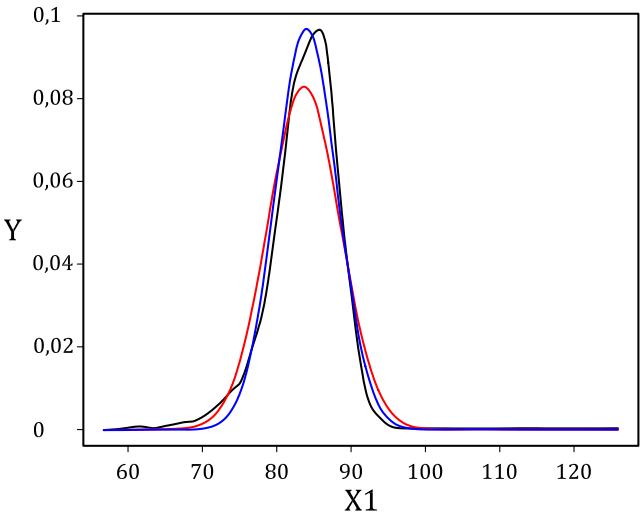

a) ECD distribution as fitted

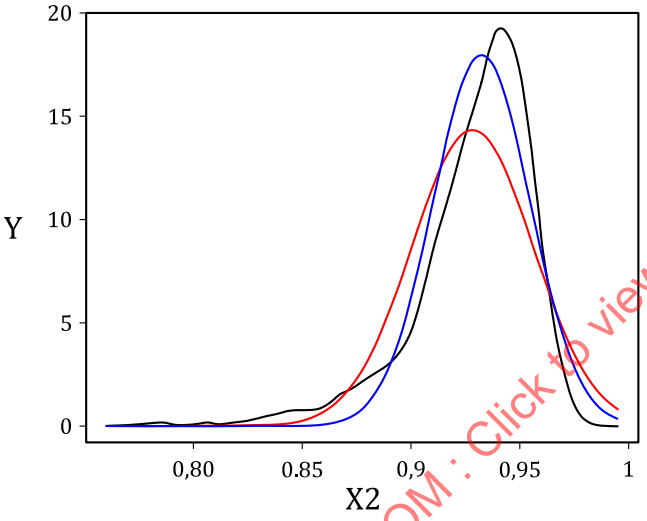

b) Aspect ratio distribution as fitted

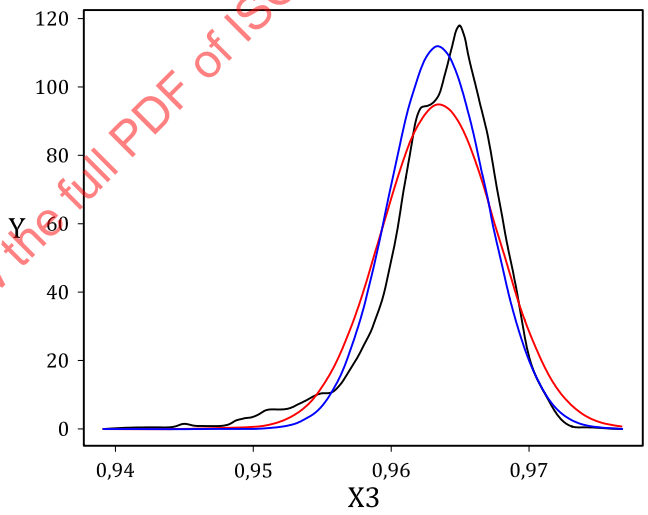

c) Solidity distribution as fitted

Key

____	smoothed density distribution of the data	X1	ECD, in nm
____	non-linear regression fit	X2	aspect ratio
____	maximum likelihood fit	X3	solidity
		Y	smoothed density distribution

Figure C.7 — Large cluster descriptor distributions fitted to normal reference model

Table C.3 shows the uncertainties associated with the three selected descriptor parameters for the separated mid-sized cluster data. Figures C.8 a) to c) show the fitted distributions with the associated data. The ECD distribution has an uncertainty of ≈5 %, and the data are significantly skewed to the left of the unimodal model curves. This is due to the fact that the data for the mid-size peak are truncated, as shown in Figures C.7 and C.8. As indicated earlier, the JRC requested the participating laboratories to report data about the large and small particle fractions only. The aspect ratio mean of the mid-sized cluster is statistically lower than that of the large cluster, i.e. the means are much more than two standard deviations distant from each other. The solidity mean of the mid-sized cluster is also statistically lower than that of the large cluster data.

Table C.3 — Separated mid-sized cluster data — Fitted parameters for the mean and spread of ECD, aspect ratio and solidity distributions (761 images) — Normal reference model

Sample	ECD nm		Aspect ratio		Solidity	
	mean	spread	mean	spread	mean	spread
D1S1	39,3	4,67	0,831	0,086 3	0,940	0,009 2
D1S2	40,4	5,83	0,837	0,096 9	0,939	0,010 8
D2S1	38,4	3,45	0,827	0,082 5	0,936	0,009 5
D2S2	38,4	3,35	0,839	0,068 8	0,937	0,009 5
D3S1	38,4	3,19	0,845	0,077 6	0,934	0,012 1
D3S2	40,0	532	0,815	0,089 5	0,938	0,011 4
average	39,2	4,30	0,832	0,083 6	0,938	0,010 4
stdev	0,896	1,13	0,010 7	0,009 7	0,002 2	0,001 2
C_v, in %	2,29	26,3	1,28	11,7	0,23	11,5
U, in %	4,95	56,8	2,77	25,2	0,50	24,7
U, value	1,94	2,44	0,023 0	0,021 1	0,004 7	0,002 6

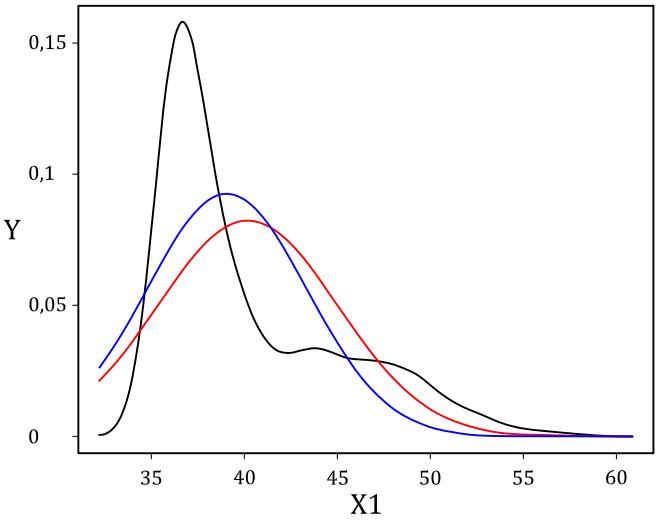

a) ECD distribution as fitted

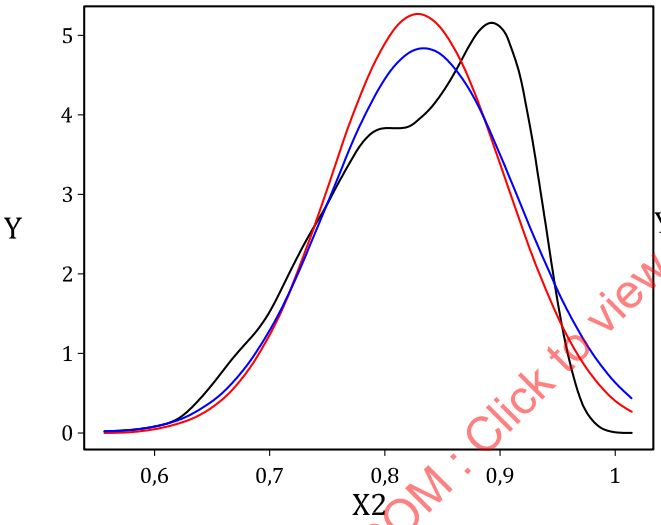

b) Aspect ratio distribution as fitted

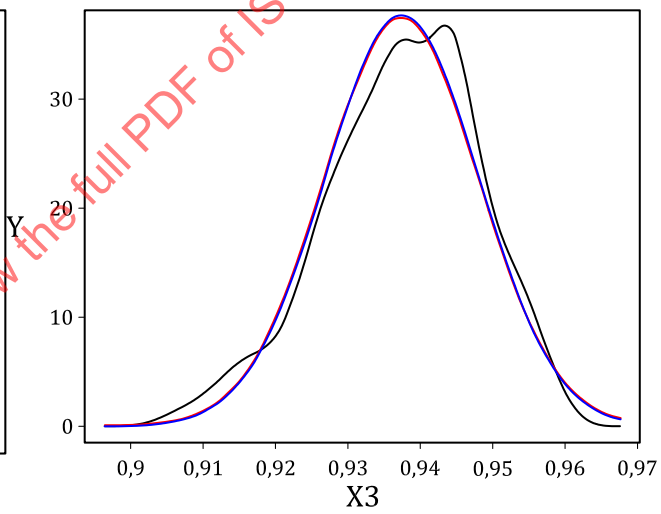

c) Solidity distribution as fitted

Key

____ smoothed density distribution of the data	X1 ECD, in nm
____ non-linear regression fit	X2 aspect ratio
____ maximum likelihood fit	X3 solidity
	Y smoothed density distribution

Figure C.8 — Mid-sized cluster descriptor distributions fitted to normal reference model

C.4 Conclusions

The Kolmogorov-Smirnov statistic is effective in determining pair-wise differences between bimodal cumulative distributions, indicating whether the two datasets are different and identifying the ranges of the data in which the highest differences occur. This method can assist investigators triaging the raw data to identify potential improvements in the protocol, i.e. elements that can lead to more repeatability, intermediate precision and/or reproducibility.

The electron microscopy data obtained on the large fraction of the ERM-FD102 mixture of colloidal silica particles can be separated into large and mid-sized clusters using a size descriptor (ECD). Bivariate plots can help visualize differences in size, elongation and ruggedness descriptors. These can enhance differentiation of cluster morphologies by illustrating which descriptors are the same, or different, between the pair. In this case, visualizations also confirm that some of the mid-sized particles have been truncated from the data or not considered. Investigators can make decisions regarding whether additional data are needed.

The aspect ratio and solidity distributions are significantly different between these two clusters and could serve as methods for differentiation. It is interesting to note that the lower point of the aspect ratio range for the mid-sized cluster, ≈0,61, is significantly lower than the similar point for the large cluster, ≈0,77. This morphology difference could be investigated further.

Annex D
(informative)

Shape mixture

D.1 Reference

The samples evaluated for this annex were provided by the National Center for Nanoscience and Technology, Beijing, China and are similar to GSB 02-2994-2013, a National Certified Standard Material in China. An ILC was used to develop a workflow for differentiating the samples[44].

D.2 Background and design objectives

The samples were made using a seed-mediated synthesis process; nanoparticle products from such processes often contain small quantities of seed particles that do not grow according to theory[49]. Figure D.1 shows an example STEM frame that shows nanorods and other shapes that are termed "nanocubes" for this document. Typically, gold nanorod sample morphologies affect their longitudinal surface plasmon residences, so it might be desirable to remove "non-nanorods" from the final product[50]. In addition, a number of particles in this frame are touching. Including touching particles during data analysis can distort descriptor distributions compared to datasets from which such complexes have been removed[26]. Users often desire automated methods for identifying, analysing and/or removing non-target particles from datasets.

The key findings of the study summarized here are:

— the method for identifying and separating touching particles (termed "complexes"), see D.3.1;

— the method for differentiating between sample morphologies, which was used to differentiate between two samples with different performance attributes (Sample 1 and Sample 2), see D.3.2.

NOTE Courtesy of Physikalisch-Technische Bundesanstalt.

Figure D.1 — A STEM image at high density of colloidal gold nanorods

D.3 Highlights

D.3.1 Method for identifying and separating touching particle complexes

A heuristic method was developed to identify descriptors and descriptor ranges that would differentiate between touching and discrete particles, and nanorods and nanocubes. Figure D.2 shows the outlines of particles from a particular frame. The 142 particles in this image were categorized with respect to being complex, discrete nanorods and discrete nanocubes. ANOVA of solidity data suggested that this descriptor could differentiate between complex and discrete particles. ANOVA of aspect ratio data suggested that this descriptor could differentiate between nanorods and nanocubes. Figure D.3 shows the bivariate plot of solidity as a function of aspect ratio for the data of Figure D.2.

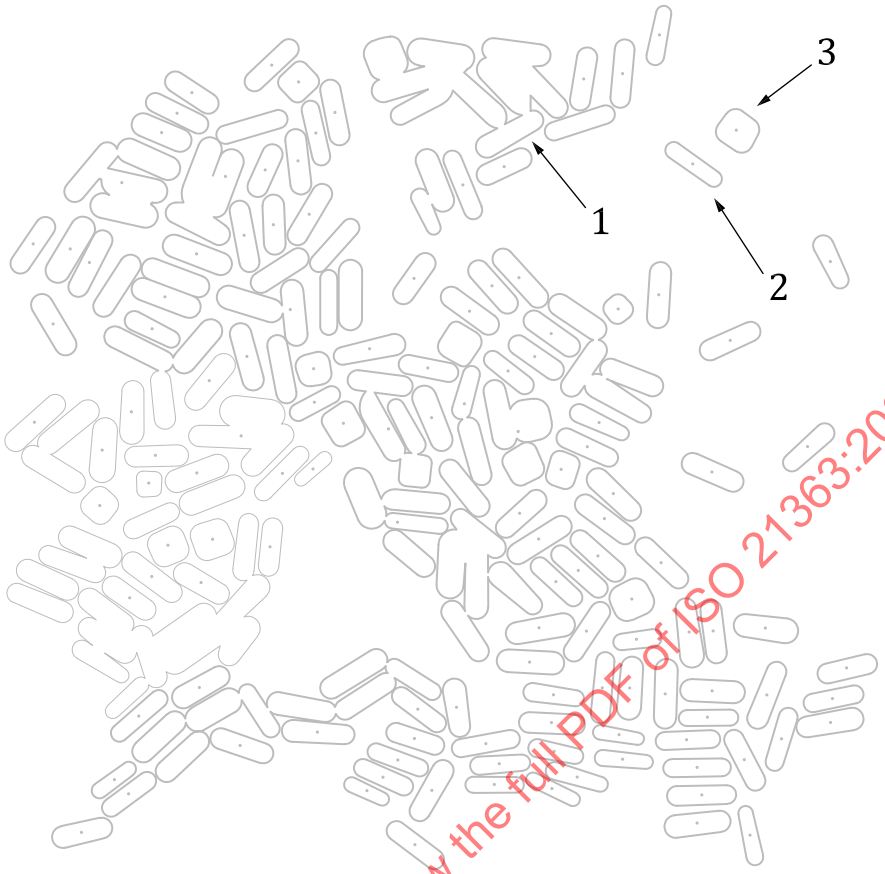

Key

1 touching particles
2 discrete nanorod
3 discrete nanocube

Figure D.2 — Image] outline drawing of gold nanoparticles on a TEM support

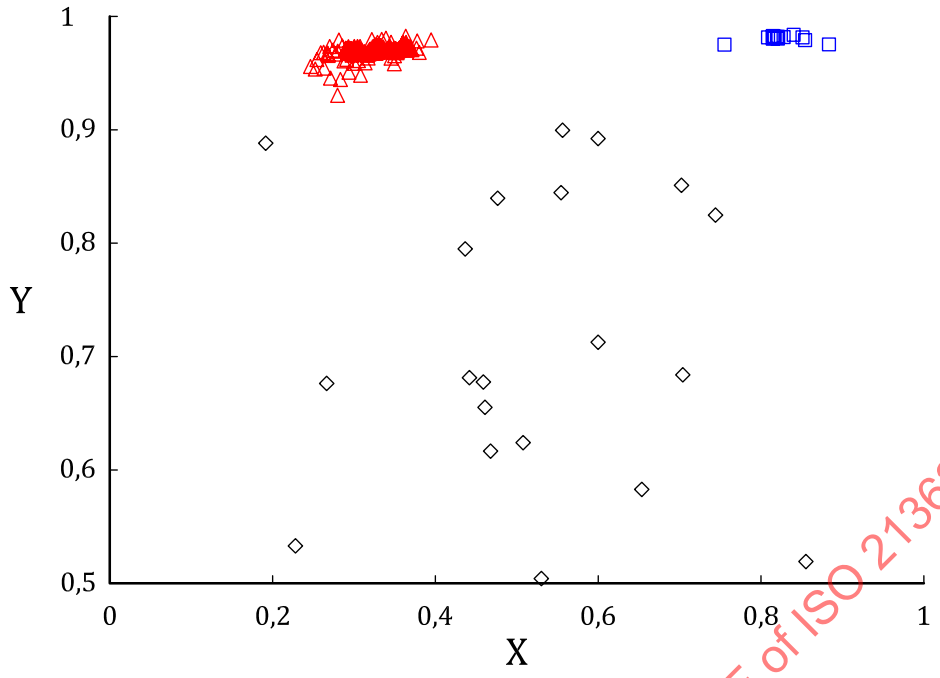

Key

□ nanocubes
△ nanorods
◇ complex structures
X aspect ratio
Y solidity

NOTE Data of Figure D.2.

Figure D.3 — Bivariate plot of solidity versus aspect ratio

Discrete nanorods and nanocubes have solidities greater than 0,9, i.e. few surface irregularities. However, their aspect ratios are distinctly different. The aspect ratios of non-nanorod particles range from 0,75 to 0,95, while the nanorods themselves have aspect ratios less than 0,5. Complex, touching particles had aspect ratios ranging from 0,2 to 0,85, but their solidities were less than 0,90. Complex particles were removed from the datasets by sorting the solidity descriptors and retaining only discrete particles for analysis. Nanocubes were separated from nanorods by sorting the aspect ratio values and retaining only the nanorod data. Since nanocube levels varied from 1 % to 4 % across the datasets, it was not practical, in this case, to develop statistics on their morphology. More nanocubes would need to be imaged for meaningful measurement uncertainties for these shapes.

D.3.2 Differentiating between nanorod samples

Table D.1 shows an ANOVA comparison of interlaboratory data for several size and elongational shape descriptors. It is clear that no size or shape means seem likely to differentiate between the samples. However, differences might be found if the spreads of distributions are considered. The distributions have different spreads, as demonstrated either by the Kolmogorov-Smirnov method, by quantile plots, or by measurement uncertainties. The grand average values of the aspect ratio spreads of Samples 1 and 2 are 0,064 9 and 0,040 6, respectively. The measurement uncertainties of these values are 5,7 % and 3,0 %, respectively, so even considering two standard deviations above and below the averages, the aspect ratio spreads are statistically different from each other.

Table D.1 — p-values of ANOVA comparison of descriptors for Samples 1 and 2[44]

Descriptor	p-values	
	Mean	Spread
Feret	0,786	< 0,001
minFeret	0,384	0,018 8
Aspect ratio	0,096	< 0,001
Compactness	0,776	< 0,001

Annex E
(informative)

Amorphous aggregates

E.1 Reference

Carbon black is an industrial material consisting of aciniform aggregates (grape-like clusters of aggregated particles). Aggregate size distribution and morphology are often used to select carbon blacks for specific applications. Cabot Corporation supplied a sample of SRB8 (see Figure E.1), an ASTM reference carbon black, for an ILC of carbon black aggregates[45].

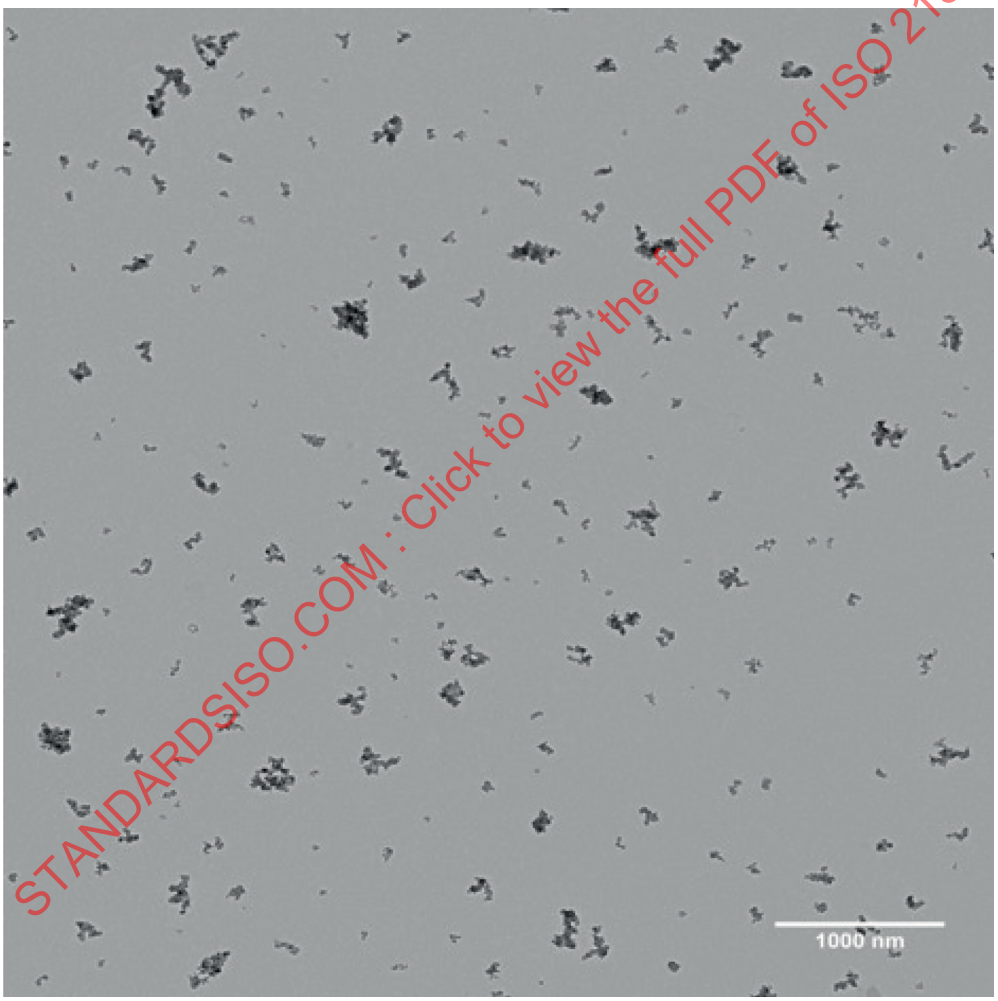

NOTE Supplied by Cabot Corporation.

Figure E.1 — Aciniform carbon black sample, SRB8

E.2 Background and design objectives

As shown in Figure E.1, there are a variety of aggregate shapes for this carbon black, which have been categorized as spheroidal, ellipsoidal, branched and linear[51][52]. An ASTM standard (ASTM D3849-14a[24]) uses two aggregate descriptors, aggregate perimeter and aggregate area, for its analysis. These descriptors provide the measurement basis for six derived parameters:

— the area-equivalent aggregate diameter;

— the aggregation factor;

— the average particle (nodule) size for a single aggregate;

— the aggregate volume;

— the particle volume;

— the number of particles in the aggregate.

In previous round-robin tests, this protocol was found to give inconsistent results, which may have resulted from descriptors associated with the aggregate perimeter. Due to the fractal nature of the aggregates, perimeter measurements are much more sensitive to image resolution than projected areas. Therefore, some key questions for the carbon black community include:

— what are the repeatabilities/reproducibilities of aggregate size and shape descriptor measurements?

— how do the different aggregate shapes impact descriptor distributions?

E.3 Highlights

E.3.1 Measurement uncertainties of carbon black aggregate descriptors

Measurement uncertainties were computed for the mean and spread parameters of reference models fitted to distribution data. Table E.1 provides measurement uncertainty estimates for conventional size and shape descriptors, plus the descriptors derived using ASTM D3849-14a (these descriptors can be used for projected area-based fractal scaling). Lognormal distribution models gave lower measurement uncertainties for size descriptors while normal distribution models gave lower measurement uncertainties for elongational and ruggedness shape descriptors. Size parameter means have measurement uncertainties of 5 % or less (except for perimeter). ECD has the lowest measurement uncertainty estimate among the size mean, which confirms it as a common choice for describing carbon black aggregate size. Elongational parameter means have measurement uncertainties less than 4 %. The solidity mean parameter has a measurement uncertainty less than 7 %. ASTM D3849-14a derived descriptor means have measurement uncertainties of 13 % and greater; these descriptors might not provide a solid foundation for descriptor correlations, such as fractal analysis.

Table E.1 — Grand means and grand spreads table for carbon black aggregate descriptors[45]

Descriptor	Reference model	Model mean	Model spread	U_{ILC} mean	U_{ILC} spread
Size					
Area, in nm^2	LN	7,75 (2 310)	1,04	4,46 %	8,77 %
Perimeter, in nm	LN	5,52 (249)	0,696	9,09 %	28,7 %
Feret, in nm	LN	4,39 (80,9)	0,586	3,55 %	6,49 %
minFeret, in nm	LN	3,94 (51,5)	0,570	4,41 %	6,18 %
ECD, in nm	LN	3,97 (52,9)	0,552	1,60 %	8,79 %
Elongation					
Aspect ratio	N	0,642	0,133	2,64 %	7,14 %
Compactness	N	0,673	0,009 8	3,24 %	14,7 %
Ruggedness					
Circularity	N	0,485	0,212	22,9 %	17,1 %
Solidity	N	0,766	0,112	6,37 %	17,8 %
ASTM D3849-14a					
d_p, in nm	LN	2,89 (18,1)	0,465	12,9 %	27,3 %
V_p, in nm^3	LN	8,03 (3 077)	1,37	14,0 %	27,3 %
N	LN	2,87 (17,6)	1,70	30,5 %	9,30 %

Key

LN = lognormal distribution model (value in brackets is exp(mean value))

N = normal distribution model

d_p = average particle size for a single aggregate

V_p = particle volume

N = number of particles (nodules) in the aggregate

E.3.2 Descriptor distributions re-assembled using four aggregate shape populations

Aggregate datasets can be deconvoluted by shape using a defined workflow[45][51]. Once all data has been categorized as spheroidal, ellipsoidal, branched and linear, descriptor distributions can be reconstructed from the contributions of their various aggregate shape components. Figures E.2 and E.3 show the reconstruction of the Feret diameter and aspect ratio distributions from aggregate shape populations. The main peak of the Feret diameter distribution is linked to its ellipsoidal aggregates. The aspect ratio distribution is multimodal. Linear aggregates contribute the most to low values of aggregate aspect ratios, while ellipsoidal aggregates contribute the most to higher aspect ratios. The deconvolution of distributions by shape might provide valuable information about the specific carbon black under study.

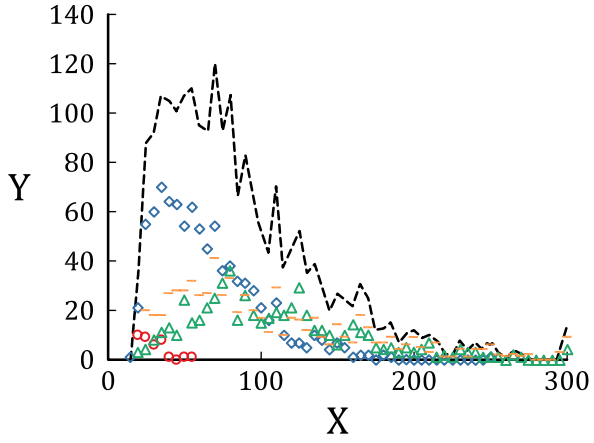

Key

- ○ spheroidal aggregates
- ◇ ellipsoidal aggregates
- △ branched aggregates
- _ linear aggregates

X Feret, in nm
Y count

Figure E.2 — Contribution of aggregate categories to the Feret distribution

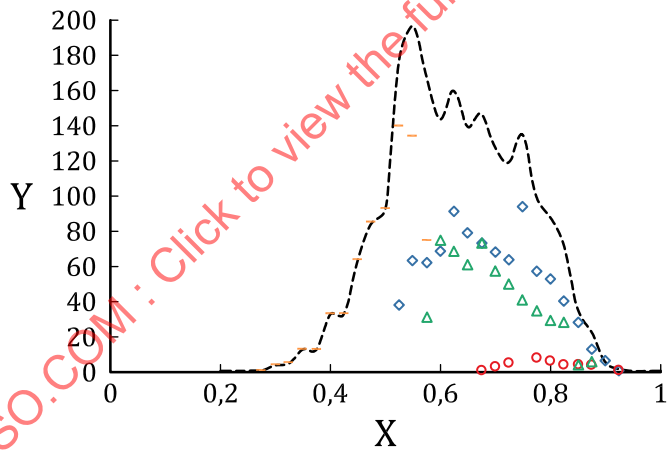

Key

- ○ spheroidal aggregates
- ◇ ellipsoidal aggregates
- △ branched aggregates
- _ linear aggregates

X Feret, in nm
Y count

Figure E.3 — Contribution of spheroidal, ellipsoidal, branched and linear aggregates to the aspect ratio distribution

Annex F
(informative)

Nanocrystalline aggregates

F.1 Reference

A sample of a commercial titania powder (MT-500BW, rutile) was supplied by Tayca[53]. Figure F.1 shows typical aggregates and a closer image of aggregated primary crystallites.

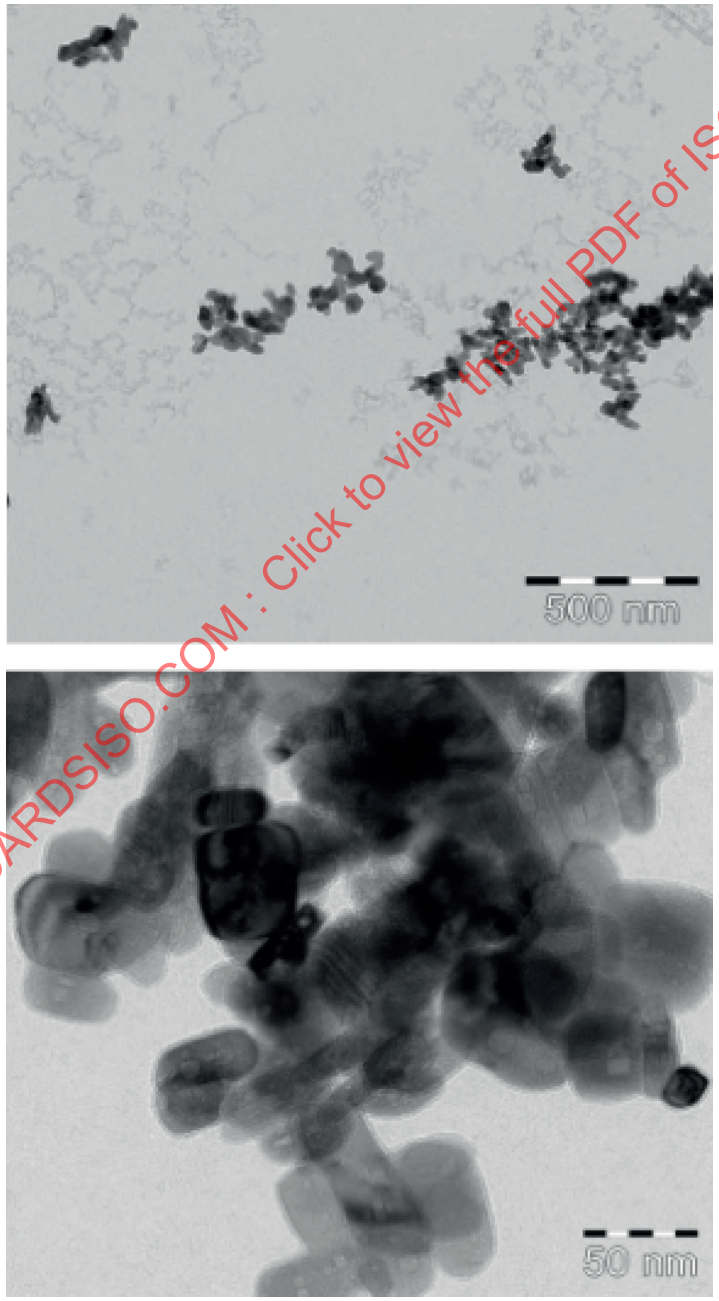

Figure F.1 — A water dispersion of titania dried on a TEM support

F.2 Background and design objectives

A number of recently proposed titania applications are linked to primary crystallite sizes within the aggregates. In this case, manual outlining of nanocrystallites is used to determine their size distribution. While the term "primary particle"[54] has been used to describe the individual elements fused together in titania aggregates, "primary crystallite" is a more precise term as there are grain boundaries between these features[55]. Details on manual outlining are provided elsewhere[53].

F.3 Highlights

F.3.1 Effects of protocol factors on crystallite data quality

Seven protocol factors were evaluated to determine their effects on data quality: laboratory, instrument type, number of particles reported, number of frames reported, calibration method, resolution (pixels per nm) and image analysis software. For the size descriptors, ECD and Feret diameter, an ANOVA of calibration methods gave a p-value greater than 0,05, suggesting that the calibration method did not affect data quality across the ILC for these descriptors. Similarly, the software used for imaging did not affect the Feret, minFeret, ECD and aspect ratio variables ($p > 0,05$). For all size descriptors, the TEM values were greater than the STEM values (differences ranged from 4 % to 7 %). The remaining factors were dependent on specific laboratories and their individual effects could not be discriminated.

F.3.2 Primary crystallite size descriptors are best modelled using lognormal distributions

F.3.2.1 General

Size descriptors of titania nanocrystallites are best modelled using lognormal distributions rather than normal distributions. Table F.1 shows the mean and spread values for each distribution applied to the ECD data. The fitted mean and spread parameters for the normal distribution have measurement uncertainties of 22 % and 31 %, respectively. However, the fitted mean and spread parameters for the lognormal distribution have measurement uncertainties of 9,5 % and 22 %, respectively. The lognormal reference model would be preferred as its U_{ILC} is less than half that of the normal model.

Table F.1 — Measurement uncertainties of ECD fitted parameters, normal and lognormal distributions

Descriptor	ECD (normal) nm		Ln(ECD), (lognormal) ln(nm)	
	mean	spread	mean	spread
Grand average, ILC	39,8	12,9	3,58	0,318
Grand st. dev., ILC	4,12	1,88	0,161	0,033
C_v, in %	10,3	14,6	4,49	10,5
U_{ILC}, in %	22	31	9,5	22

F.3.2.2 Data visualizations complement measurement uncertainty values

The normal distribution or the Weibull distribution can be used to fit aspect ratio data. Figure F.2 shows that the aspect ratio distribution for Lab 1 data is multimodal.

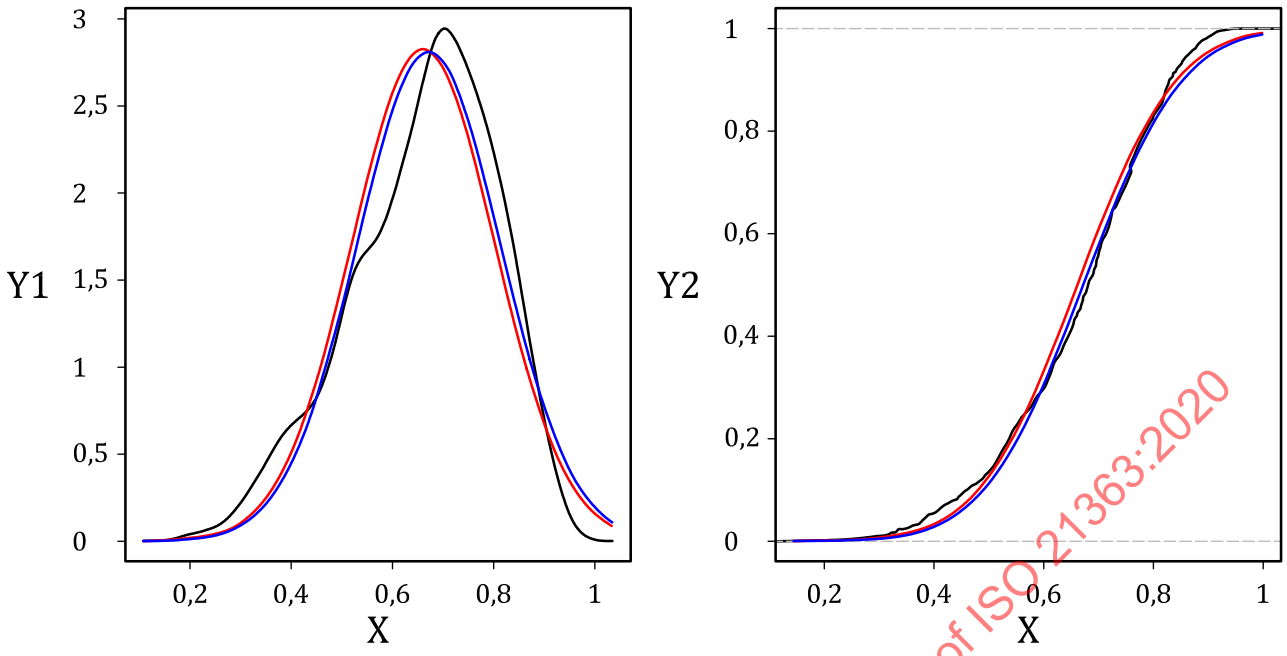

a) Aspect ratio density distribution **b) Aspect ratio cumulative distribution**

Key

____	smoothed density distribution of the data	X	aspect ratio
____	non-linear regression fit	Y1	smoother histogram
____	maximum likelihood fit	Y2	cumulative distribution

Figure F.2 — Density and cumulative distributions of aspect ratio (Lab 1)

A bimodal model can be fitted to these data; this requires five fitted parameters. Figure F.3 shows the residual deviation plots for the unimodal normal fit, the unimodal Weibull fit and a bimodal Weibull fit to the aspect ratio data. For the data of this laboratory, the residual deviation plot suggests that the Weibull distribution should be preferred over the normal distribution, and that the Weibull bimodal distribution fits the data over a much larger range of aspect ratios. The mean value of the aspect ratio is shown as a red vertical line. The unimodal and bimodal Weibull models are closer to the data near its average value, and the bimodal Weibull fit is closer to the data over a wider range than either of the other models.

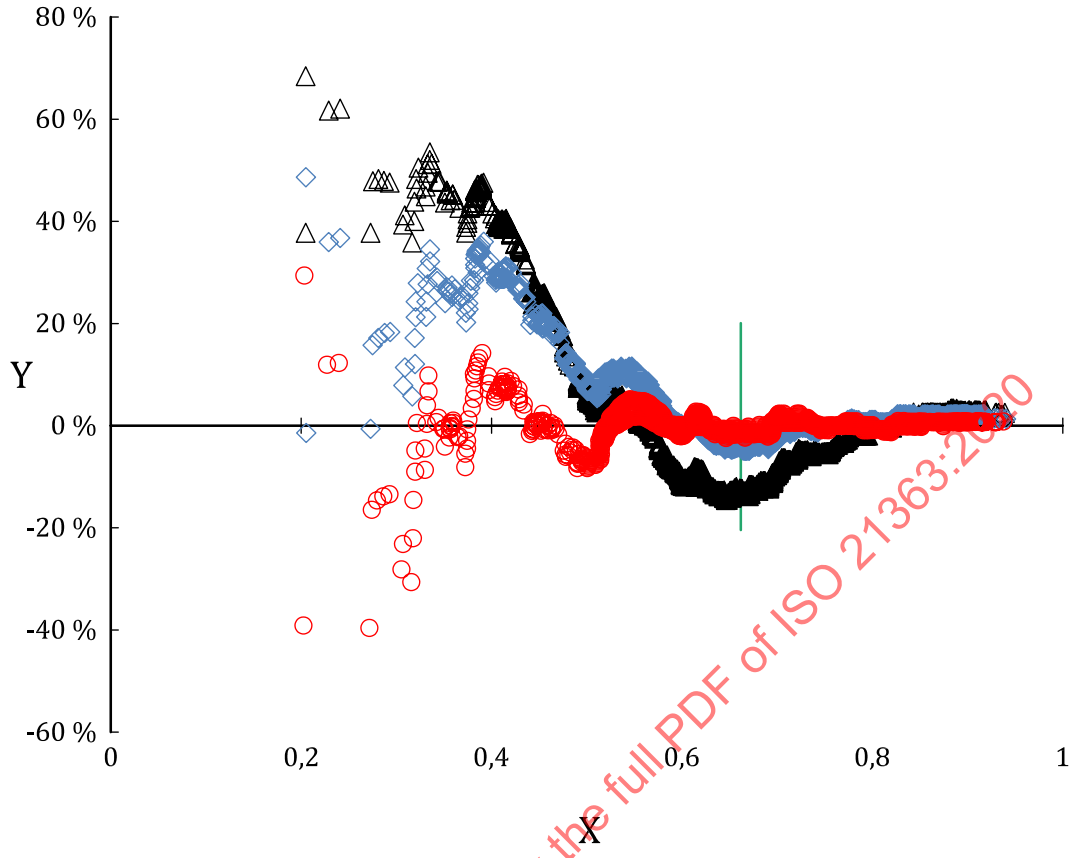

Key

△ normal distribution
◇ Weibull distribution
○ bimodal Weibull
aspect ratio mean

X aspect ratio
Y relative residual deviation, in %

Figure F.3 — Normal, Weibull and bimodal Weibull fits to an aspect ratio distribution (Lab 1)

Annex G
(informative)

Nanofibres with irregular cross-sections

G.1 Reference

The samples evaluated for this annex, cellulose nanocrystals (CNCs), were provided by National Research Council Canada/Conseil R de recherches Canada (NRC) and are based on a CRM[46]. All procedures were developed and tested in-house[56], and a number of commercial samples of these materials are available[57].

G.2 Background and design objectives

This commercial material (provided courtesy of CelluForce Inc., Windsor QC) was produced by sulfuric acid hydrolysis of softwood pulp and purified by neutralization, sodium exchange, purification and spray drying. Negatively-charged surface groups remain in their surfaces, but can help stabilize aqueous colloidal suspensions[56]. Sulfated CNCs have been reported to have average length/width ratios of 11 to 12[58], which correspond to aspect ratios of 0,083 to 0,091. Since amorphous cellulosic regions are degraded during the acid hydrolysis process[59], the nanoparticles can be highly crystalline with high axial moduli and crystal stiffness[60]. As shown in Figure G.1, CNCs of this sample often have two dimensions in the nanoscale (widths in the range of 1 nm to 100 nm) and lengths of 100 nm and longer, meeting the definition of nanofibres (see 3.1.9). Unlike gold nanorods (see Annex D), which have uniform widths perpendicular to their length axis, CNCs have irregular widths along their length axis.

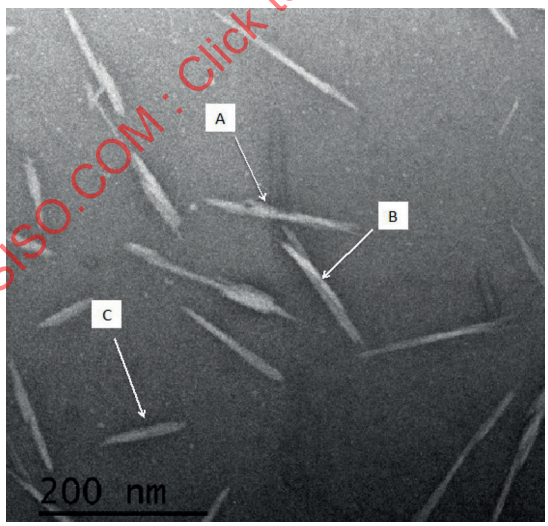

Key

Object A possible CNC aggregate or agglomerate
Object B agglomerate of two discrete CNC nanofibres
Object C discrete CNC nanofibre

NOTE Courtesy of NRC Canada.

Figure G.1 — Cellulose nanocrystal particles